Stratigraphic Architecture, Depositional Systems, and Lithofacies of the Mississippian Upper Barnett Two Finger Sand Interval, Midland Basin, Texas

Justin V. Mauck[1], Robert G. Loucks[1], and David J. Entzminger[2]

[1]*Bureau of Economic Geology, Jackson School of Geosciences, University of Texas at Austin, University Station, Box X, Austin, Texas 78713–8924, U.S.A.*

[2]*Entzminger Geoscience Services, LLC, 5606 Ridgemont Pl., Midland, Texas 79707, U.S.A.*

ABSTRACT

The upper Barnett Two Finger Sand interval in West Texas forms oil and gas reservoirs that produce from natural fractures and low-permeability intraparticle nano- to micropores in the matrix. The section contains two mixed medium silt- to very fine sand-sized siliciclastic-carbonate units that are composed of relatively thin 0.5 mm to 1 m hybrid/cogenetic event beds that amalgamate to form a deepwater submarine fan system in the Mississippian Tobosa Basin. Siliceous mudstones occur between these coarser-grained units. Sediment sources for the fan lobes originated from the northern and eastern margins of the Tobosa Basin in an inner ramp setting. The depositional setting, based on elevated total organic carbon (up to 3.1%), lack of wave-related hydrodynamic features, and the presence of cephalopods and radiolarians, is interpreted as having been below storm-wave base in a generally dysaerobic outer ramp to basin bottom water setting with brief periods of oxygenation. Most of the organic matter is type III, but a minor amount of type II organic matter is present. Calculated vitrinite reflectance (R_o) values average 1.2%, which places the Two Finger Sand interval within the late oil to early gas window. Core-plug porosity ranges from 0.5 to 7.5% with permeability generally less than 0.06 md. Pore types include intraparticle fluid-inclusion pores and clay-platelet mineral pores. Some microvugs (<1 to 10 μm) are observed that may be related to dissolution. Rare organic-matter pores are present. Based on decline curves from producing wells and shut-in pressure tests performed during the development of the Moonlight Field, it was concluded that the permeability network in the reservoir consists of natural fractures. After a few years of production, however, the decline curves suggest that some production is from the matrix. The concepts developed concerning the depositional setting and sediment-source areas and sediment flow directions may aid in the development and extension of the Two Finger Sand interval play.

INTRODUCTION

The Barnett Shale in southeastern New Mexico and West Texas was deposited during Mississippian Osagean-Chesterian time (Fig. 1) in the deeper-water area of the Tobosa Basin (Hamilton and Asquith, 2000; Broadhead, 2006; Osterlund, 2012). Siliciclastic muds were the predominant sediment deposited in the basin except for several intervals composed of coarser mixed siliciclastic-carbonate gravity-flow deposits. These mixed siliciclastic-carbonate gravity-flow-dominated units are referred to as the Two Finger Sand interval based on their upward-coarsening, high to low gamma-ray log expression (Fig. 2). The Two Finger Sand interval has a long history of oil production in

Midland and Andrews counties (Candelaria, 1990; Osterlund, 2012; Entzminger, 2015).

The major goal of this investigation is to provide the depositional history of the Two Finger Sand interval. Specific objectives include the following: (1) construct the regional paleogeographic setting and associated stratigraphic architecture of the upper Barnett interval; (2) map the lateral extent of the Two Finger Sand interval sand bodies; (3) define the lithofacies within the upper Barnett interval; (4) propose the origin of the Two Finger Sand interval, the source of sediments, and range of depositional processes that constructed the sand bodies; and (5) describe the reservoir characteristics of the Two Finger Sand interval sand bodies.

DATA AND METHODS

The major sources of data for the upper Barnett Two Finger Sand interval are wireline logs and cores from Midland and Andrews counties (Table 1; Fig. 3). A Petra® database was constructed using 364 wireline logs. Tops were picked for the

Figure 1. Stratigraphic column showing Devonian through Lower Pennsylvanian strata in West Texas and New Mexico (Meyer, 2002; Ruppel and Kane, 2007). The Two Finger Sand interval was deposited during the Meramecian to Chesterian stages (~330 Ma). Modified sea-level curve from Ross and Ross (1987) indicates third-order sea-level fluctuations during this time period.
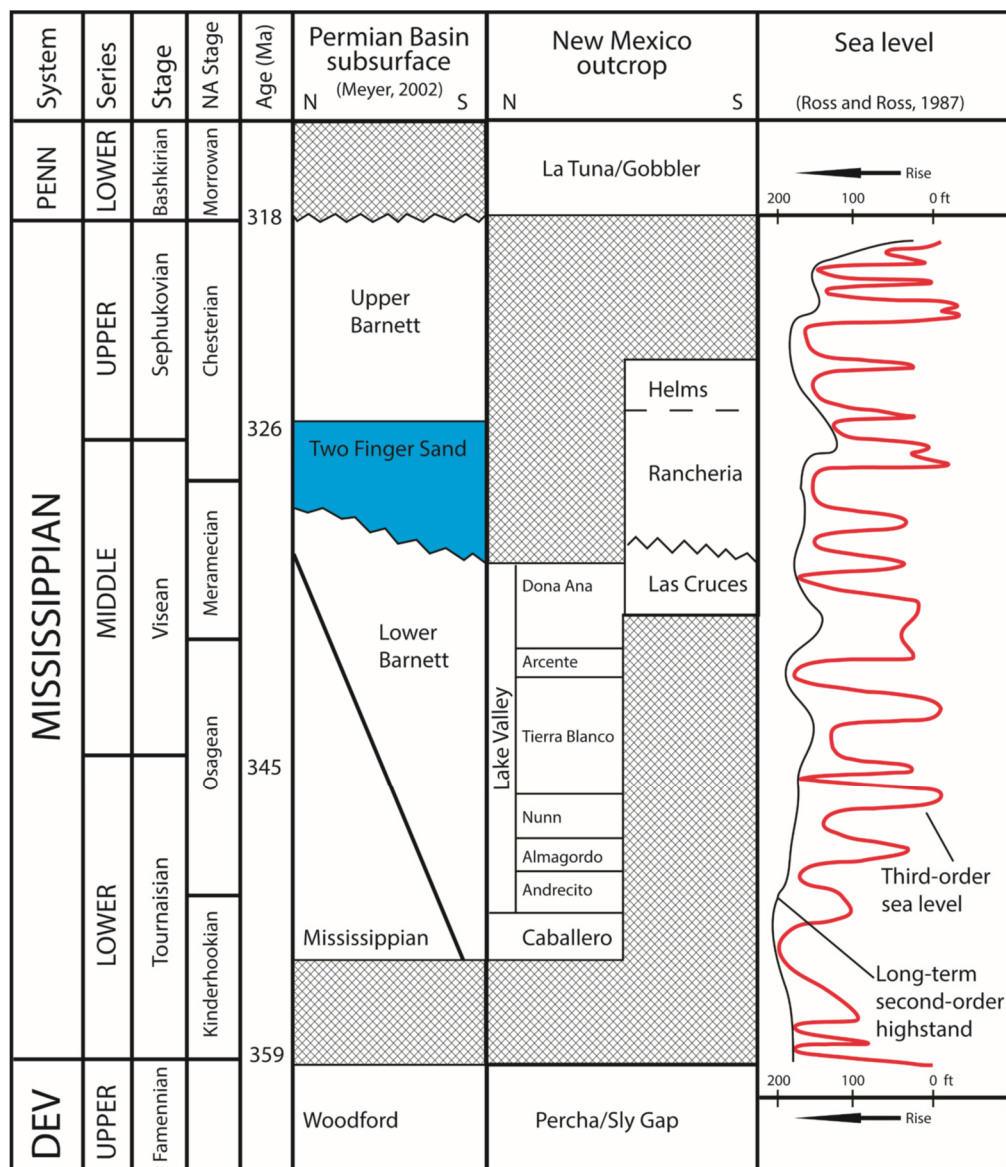
Mississippian Lime, Lower Barnett, Lower Two Finger Sand, Upper Two Finger Sand, Upper Barnett, Atoka Lime, and Strawn (Fig. 2). The tops were used to create cross sections that identified the stratal geometry of the units and to create isopach maps to identify the lateral extent and trends of the Two Finger Sand interval and its configuration.

Seventy-seven polished thin sections were prepared to identify finer sedimentary features, rock texture, fabric, mineralogy, and biotic components (prepared by National Petrographic Services, Inc., Houston, Texas). Thin sections were impregnated with UV–epifluorescence dye to emphasize micropores under mercury-vapor light on the petrographic microscope.

Eight samples were examined for mm-scale texture, fabric, organic matter, and pores using a field-emission scanning electron microscope (FESEM) (FEI Nova NanoSEM 430 at the University of Texas at Austin). Energy dispersive spectroscopy (EDS) was used construct elemental maps to identify mineralogy. Four polished thin sections with a 4 nm carbon coating were examined on the FESEM , which provided acceptable results for recognizing pores and identifying mineral constituents. Other samples imaged were prepared using Ar–ion milling techniques (Reed and Loucks, 2007; Loucks et al., 2009).

X–ray diffraction (XRD) analysis was completed on five samples by Weatherford Laboratories in Houston, Texas, and by K–T GeoServices, Inc., in Gunnison, Colorado. Mineralogy was provided by percent weight (Fig. 4).

Energy dispersive X–ray fluorescence (XRF) data were collected on all seven cores using a Bruker Tracer III handheld XRF unit equipped with an RH X–ray tube. Analyses were run at a 2 in sampling interval. The core was scanned for both major and trace elements spectra. The minor element spectra were collected at 40 kV and 25 μA, for 90 sec under ambient conditions. The major element spectra were collected at 15 kV and 34.4 μA for 60 sec under a vacuum.

Thirty-six samples from two wells, mainly from dark siliciclastic mudstones, were selected for total organic carbon (TOC) and Rock-Eval® analysis. The samples were analyzed by GeoMark Research, Ltd., in Houston, Texas.

Fifteen 1 in horizontal plugs were taken from two wells for conventional porosity and permeability analysis, and 58 porosity and permeability measurements were provided by Fasken Oil & Ranch, Ltd., in Midland, Texas. The plugs were analyzed by Weatherford Laboratories in Midland, Texas. Samples were chosen to analyze a spectrum of rock types.
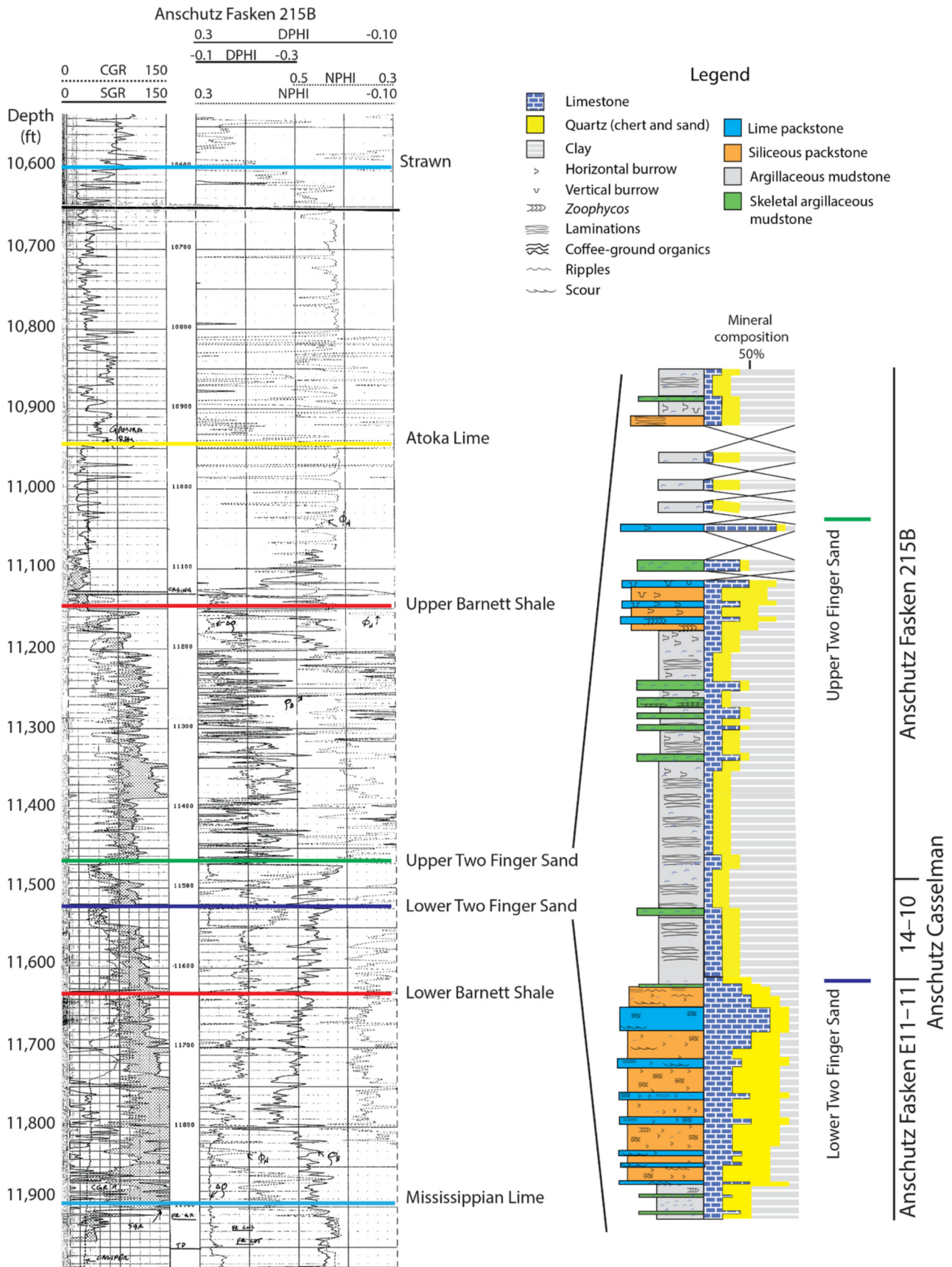
Figure 2. Type section for the Two Finger Sand interval in the upper Barnett section, and composite core description from a combination of the Anschutz Fasken 215B and Anschutz Casselman 14–10 wells for the upper Two Finger Sand and the Anschutz Fasken E11–11 well for the Lower Two Finger Sand (Midland County, Texas). Log curves: SGR, standard gamma ray; CGR, computed gamma ray; DPHI, density porosity (limestone matrix, 2.71 g/cm^3, and fluid density, 1.00 g/cm^3); and NPHI, neutron porosity (limestone matrix units).

Table 1. Cores used in this study documenting top burial depth and core thickness.

| Well name	Well code	API	County	Feet of core	Top burial depth (ft)
Exxon Fasken	Block B#1	42003355520000	Andrews	59	11,612
Anschutz Casselman	14–10	42329314680000	Midland	46	11,510
Anschutz Fasken	E11–11	42329315130000	Midland	27	11,489
Anschutz Fasken	6–13	42329315140000	Midland	40	11,496
Anschutz Fasken	10–19	42329311810000	Midland	26	11,580
Anschutz	C11–11	42329315310000	Midland	19	11,442
Anschutz Fasken	215B	42329314020000	Midland	90	11,450
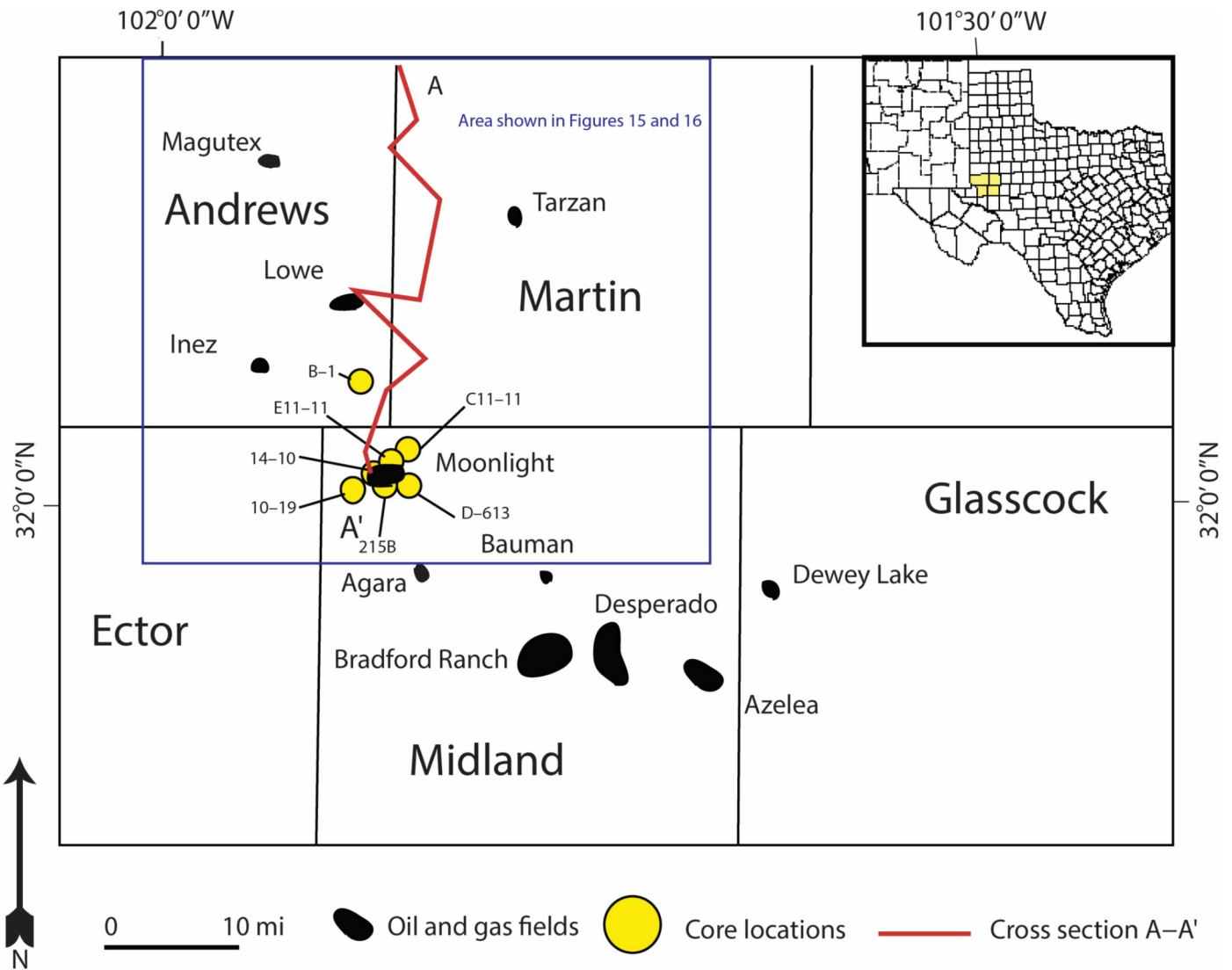
Figure 3. Map showing the location of cores in Midland and Andrews counties. Base map modified after Osterlund (2012). Locations of Two Finger Sand fields and cross section A–A' are also presented. 10 mi = ~16 km.

GEOLOGIC SETTING

The Tobosa Basin formed during Late Cambrian to the Late Mississippian where a persistent sag occurred along the continental margin of Laurussia (Miall, 2008). The Tobosa Basin is approximately 300 mi (480 km) in length along the northwest-trending central axis and 290 mi (460 km) wide. The basin is asymmetric, with thicker sediment accumulations to the west and thinner deposits to the east. The northern slope of the Tobosa

Basin during the Late Mississippian, based on analyses of wire-line log cross sections, dipped at 0.16–0.17° from the inner-ramp to the basin floor. During the Mississippian, the basin was bounded by the Texas Arch and Dickens Trough to the northeast (Fig. 5). The Tobosa Basin accumulated approximately 7000 ft (~2330 m) of sediment (uncompacted) at the western edge during its existence (Adams, 1965).

During the Mississippian Period (Osagean to Chesterian), the Tobosa Basin was juxtaposed with a broad, shallow-water
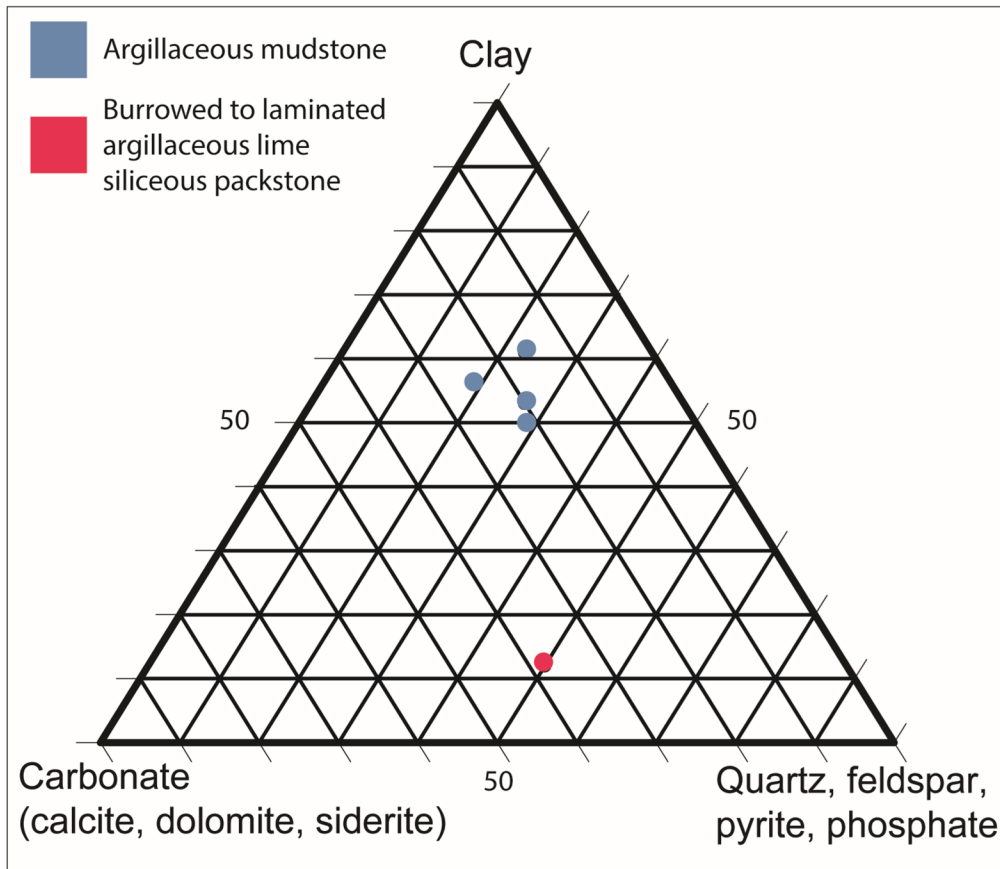
Figure 4. XRD ternary diagram of Two Finger Sand mineralogy by lithofacies.
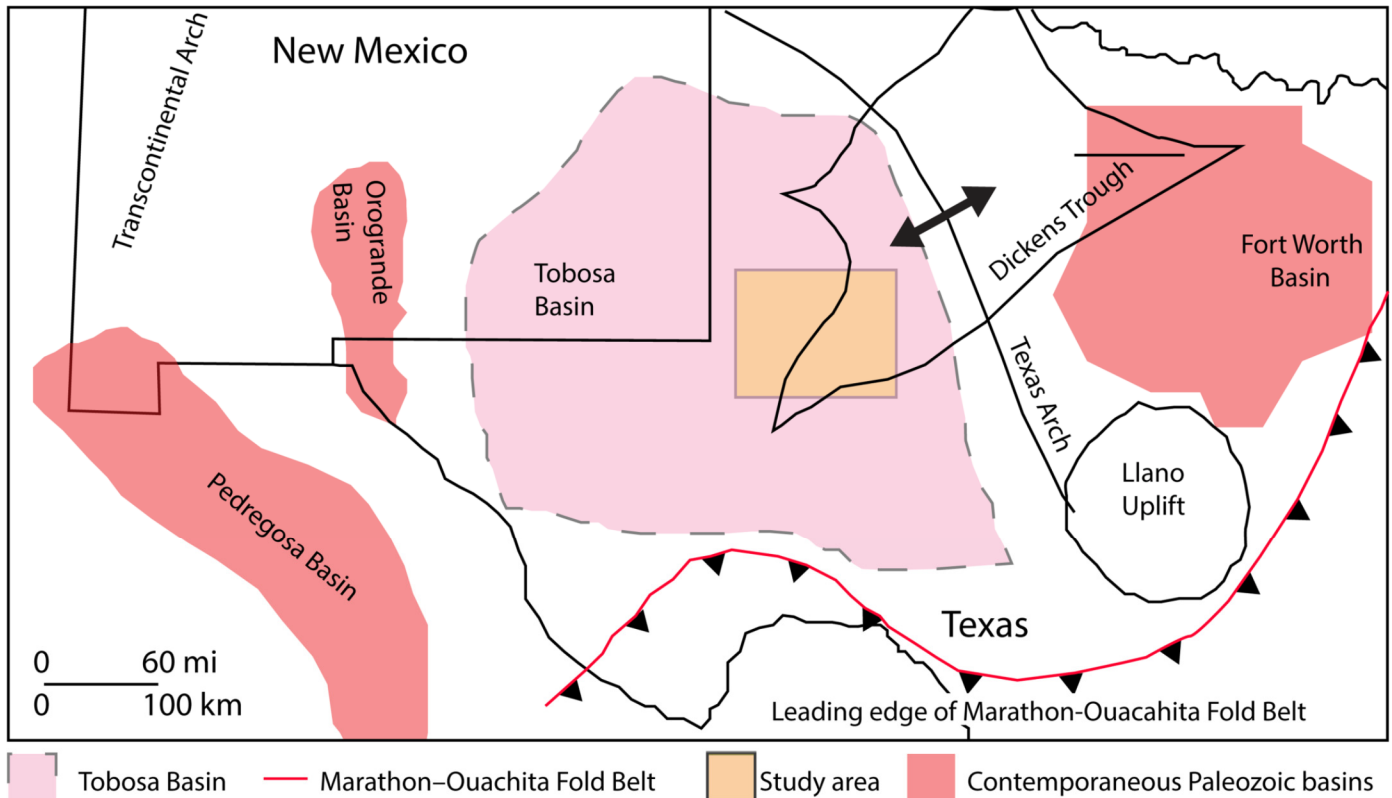

Figure 5. Paleotectonic elements present during the time of Two Finger Sand deposition in the Tobosa Basin; the most influential structure was the Texas Arch (modified after Craig and Connor, 1979; Frenzel et al., 1988). A broad, shallow carbonate ramp developed along a broad bulge that paralleled the Ouachita Orogeny (Craig and Connor, 1979; Ettensohn, 1993; Hamilton and Asquith, 2000).

carbonate platform that occupied most of the southern and western margins of Laurussia. The northern portion of the Tobosa Basin carbonate ramp was composed of arid tidal flats, intertidal channels, and oolitic shoals (Fig. 6) that formed on a broad bulge that paralleled the Ouachita Orogeny (Craig and Connor, 1979; Ettensohn, 1993; Hamilton and Asquith, 2000). Ooid generation reached maximum production levels during the Meramecian (Ettensohn, 1993). Biota included algae, fenestrate bryozoans, trilobites, brachiopods, ostracods, benthic foraminifera, and crinoids (Ruppel, 1985; Hamilton and Asquith, 2000; Sivils, 2004; Krainer and Lucas, 2012). Bioherms nucleated along the middle to outer ramp (Laudon and Bowsher, 1941; Gutschick and Sandberg, 1983; Frenzel et al., 1988). During the Late Mississippian, the topographic high associated with the northward movement of the Ouachita Orogeny increased restriction of bottom-water circulation (Noble, 1993; Rowe et al., 2008).

Paleogeographic reconstructions (Blakey, 2005; Ruppel and Kane, 2007) define a carbonate ramp occupying a broad region that was strongly influenced by the Texas Arch. Proximal calcareous sediments were transported from the north down the carbonate ramp by mass gravity-flow transport (Fig. 6), (Yurewicz, 1977; Loucks and Ruppel, 2007). Distal, deeper-water sediments were supplied by hemipelagic sediments and some biota from the water column such as radiolarians and cephalopods (Ruppel and Kane, 2007). The Barnett Formation reaches a thickness greater than 2000 ft (~610 m) in the western portion of the Tobosa Basin and 300 ft (~91 m) in the eastern area (Frenzel et al., 1988).

The Barnett Shale in southeastern New Mexico and West Texas was deposited during the Mississippian Period (Osagean to Chesterian) in a basinal setting (Lane, 1974; Hamilton and Asquith, 2000; Broadhead, 2006; Ruppel and Kane, 2007; Osterlund, 2012). Deposition was below both storm-wave base and oxygen-minimum zone (OMZ) (Gutschick and Sandberg, 1983; Ruppel and Kane, 2007; Miall, 2008). A modified sea-level curve (Fig. 1) suggests that Barnett deposition occurred during a second-order sea-level highstand with a number of third-order sea-level fluctuations (Ross and Ross, 1987; Loucks and Ruppel, 2007). Considering the magnitude of relative sea-level fluctuations (up to 150 ft [~45 m]) proposed by Ross and Ross (1987), water depth within the basin was probably greater than 450 ft (~137 m) in order to not have been overturned by deep storm waves (Loucks and Ruppel, 2007).

During the Late Mississippian, widespread erosion of the older Mississippian section was documented in Texas and New Mexico (Gutschick and Sandberg, 1983). This was caused by the constructive interference of the Antler and Ouachita orogenic bulges (Ettensohn, 1993). As a result, in the western portion of the study area, much of the Mississippian section is missing.

During Early Pennsylvanian, the Tobosa Basin was broken up into the present-day tectonic features of the Permian Basin (Fig. 7). Uplift of the Central Basin Platform produced a prominent positive structural element that separated the Midland and Delaware Basins and caused associated widespread erosion of pre-Pennsylvanian strata on the platform. The Bend Arch separated the subsiding Midland and Fort Worth basins (Frenzel et al., 1988).

LITHOFACIES

In this study, five lithofacies were recognized in the Two Finger Sand interval on the basis of mineralogy, biota, and texture: (1) burrowed to laminated lime argillaceous siliceous packstone; (2) burrowed to laminated siliceous lime packstone; (3) argillaceous mudstone; (4) argillaceous skeletal wackestone to packstone; and (5) skeletal grainstone. Two Finger Sand interval lithofacies were defined using core and thin-section descriptions from seven wells (Table 1), thin sections (Figs. 8–12), and XRF and XRD analyses (Fig. 4).

Burrowed to Laminated Lime Argillaceous Siliceous Packstone

Burrowed to laminated lime argillaceous siliceous packstone (Fig. 8) is the dominant lithofacies within the Two Finger Sand interval. Fabric ranges from burrowed to well laminated. Burrows are common throughout the cores in this lithofacies and diminish toward the top of each packstone unit. Burrow traces are *Zoophycos*, *Chondrites*, and *Planolites* (Figs. 8A and 8B). Textural components are medium to coarse silt-sized chert grains, peloids, and highly-fragmented skeletal material. The most common siliceous grain type is microporous chert (Figs. 8C–8F). Peloids are commonly compacted and form a clotted fabric. Skeletal material is composed of fragmented sponge spicules, crinoids, bivalves, and brachiopods. Most of these components are interpreted to have been transported into the deeper parts of the basin. Glauconite and organic matter are minor constituents, as well as authigenic pyrite. Pyrite is present as framboids ranging from 1 to 10 µm and as euhedral crystals replacing carbonate grains.

The sediment is well compacted. Remaining interparticle pores appear to be occluded with calcite and dolomite cement. The only pore types observed are intraparticle micropores developed within the chert and carbonate skeletal grains (Fig. 8E). These types of pore networks are associated with very low measured permeability values (<0.06 md).

The laminations in fine-grained sediment are preserved where burrows did not disrupt the original sediment fabric. Some of these laminae show mm-scale alterations of silt- to clay-sized dominated laminae with upward-fining cycles and are probably the result of waning flow-current processes. Ripples and water-escape features associated with these laminations are common throughout the upper portion of the packstone units. These laminations are highlighted by broken skeletal material and coffee-ground organic matter (flakes of compressed wood chips, leaves, pollen, etc.) that align parallel to bedding (Fig. 8C). The sediments were deposited primarily in a dysaerobic to anaerobic environment, evidenced by horizontal burrows and their lack of deep penetration into the underlying sediment and laminations, as well as fair to excellent TOC values ranging from 0.62 to 3.1%.

Burrowed to Laminated Siliceous Lime Packstone

Burrowed to laminated siliceous lime packstone is found throughout the Two Finger Sand interval (Fig. 9). These deposits range in thickness from less than 6 in (~0.15 m) to 2.5 ft (~0.75 m). Rock fabric varies from ripple-laminated upward-fining sequences to burrowed (Figs. 9A and 9B). Burrow traces are *Zoophycos* (Fig. 9C), *Chondrites*, and *Planolites*. Textural components in this lithofacies are oolitic coated grains, peloids, and fragmented skeletal grains (Fig. 9D).

According to EDS point counting for the primary mineral composition, calcite comprises 33.6%, dolomite 14.2%, quartz 30%, and glauconite 19.8%. Minor amounts of illite (1%) and organic matter (<1.2%) are present (Fig. 9E). Clay minerals are generally dispersed throughout this lithofacies and appear in greater concentrations within the ripple laminations that cap the upward-fining sequences (Fig. 9A). The dispersed clays are commonly associated with organic matter and burrows. TOC values range from 1.0 to 1.2%.

Burial compaction of the clays has reduced the thickness of clay-rich layers by 65 to 80%, as is well displayed by clay compaction around rigid skeletal fragments (Fig. 9F). Interparticle pores are entirely filled with calcite and dolomite cements (Fig. 9D). Micropores are present within the calcite, glauconite, and peloidal grains. This lithofacies has a low porosity of 0.4 to 4.0% and <0.04 md permeability. Laminae sets in this lithofacies range up to 0.005 in (125 µm) (Fig. 9B) and are composed of interbedded layers of carbonate and quartz grains, with minor
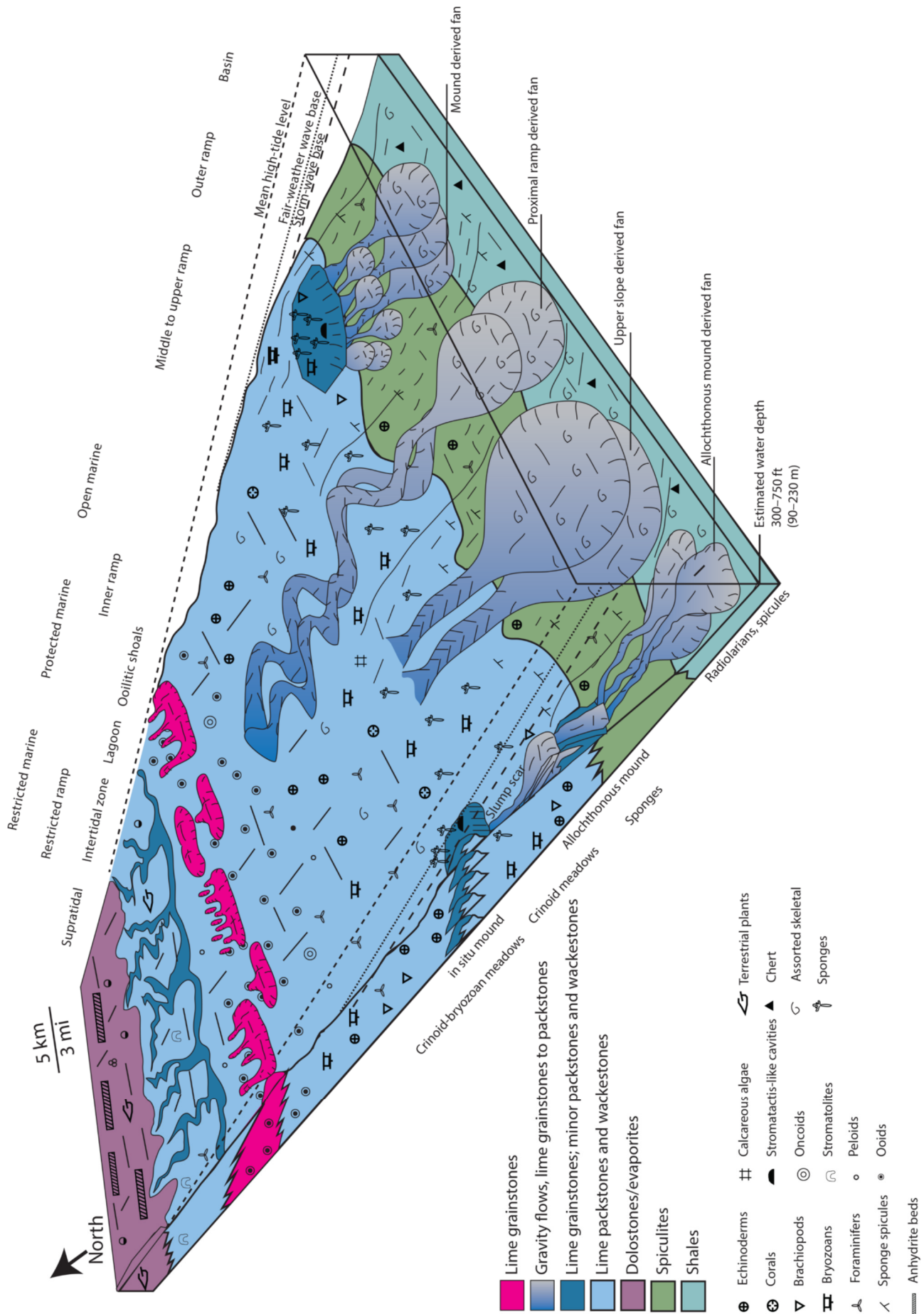
Figure 6. Idealized three-dimensional depositional model (modified after Armstrong and Mamet, 1988). Two Finger Sand deposition occurred below storm-wave base in the distal outer ramp to basinal setting. Shallow-water components were sourced from updip in the proximal ramp setting.
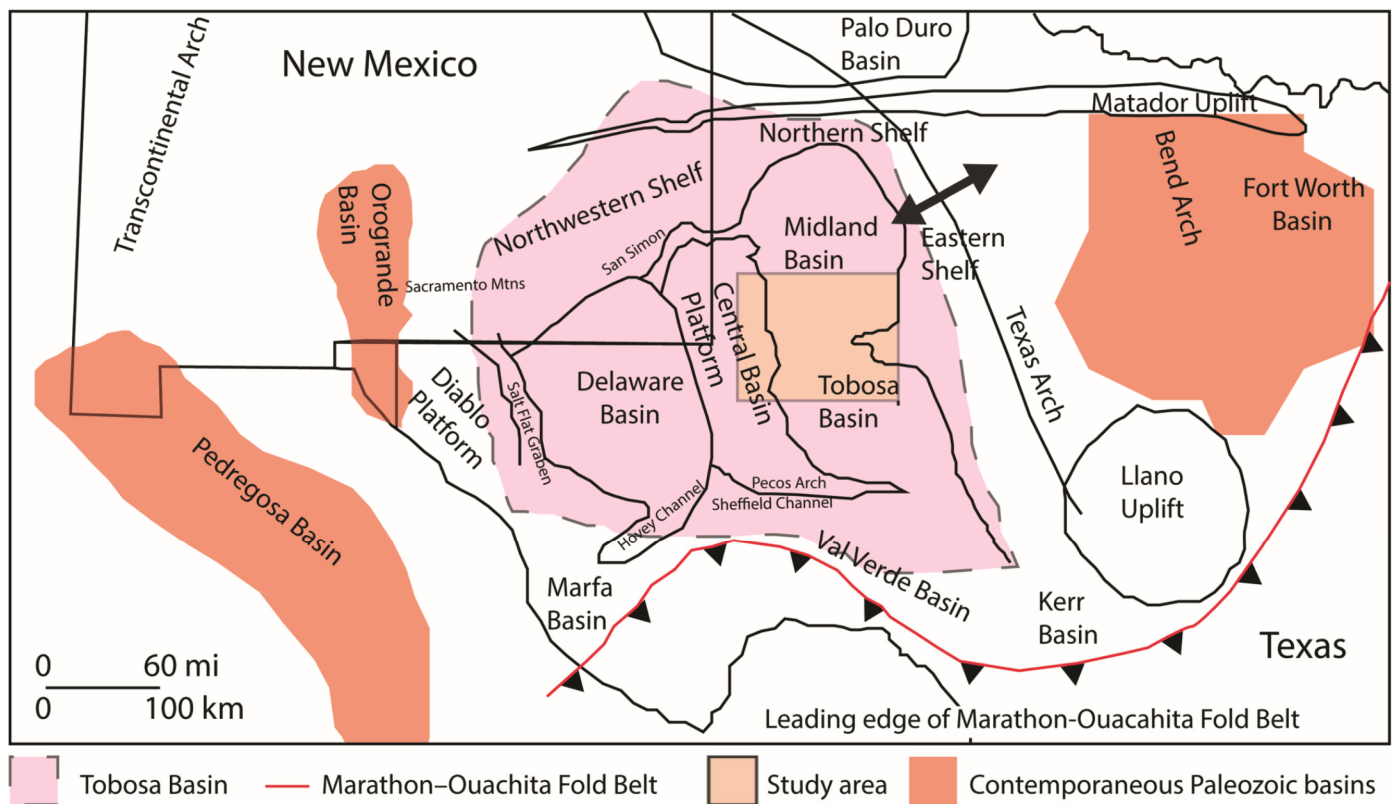
Figure 7. Post-depositional tectonic elements (modified after Frenzel et al., 1988). Tectonic activity reached a peak in the Middle Pennsylvanian.

amounts of clay (Fig. 9E) and organic matter (Fig. 9F). This lithofacies is composed of relatively thin 0.02 in to 3 ft (~0.5 mm to 1 m) hybrid/cogenetic event beds that get thicker towards the top of each sand unit. These gravity-flow units brought oxygenated waters with sediment containing shallow-water faunal components into the deeper-water area of the Tobosa Basin.

Argillaceous Mudstone

Argillaceous mudstones (Fig. 10) consist of very fine-grained mud composed mainly of clay minerals (kaolinite, illite, and mixed-layer illite/smectite, with minor chlorite), quartz, and carbonate. According to XRD analysis (Fig. 4), clay minerals comprise 55% of this lithofacies. Carbonate comprises 20% and includes predominantly calcite, with minor ferroan dolomite and siderite. Quartz content averages 20% and includes chert and megaquartz replacement of brachiopod shells (Figs. 10A and 10B). Pyrite is also present in trace amounts as framboids (<2 μm) and euhedral pyrite crystals replaced foraminifera tests and echinoid spines (Figs. 10D and 10E). Textural components in this lithofacies are peloids, quartz grains, and both in situ and transported fauna. Skeletal debris includes brachiopods, crinoids, foraminifera, and bivalves. The dominant grain size of carbonate and quartz ranges between 5 and 10 μm (clay to very fine silt).

Similar to the Barnett Formation in the Fort Worth Basin (Loucks and Ruppel, 2007), there is a presence of chert and plagioclase (albite) (Fig. 10F). To the northeast and north, the Tobosa Basin was dominated by shallow-water carbonate deposition. These areas are unlikely the source of the terrigenous material. Some of the terrigenous sediments are possibly sourced from the Caballos Arkansas Island chain to the southeast. Gutschick and Sandberg (1983) documented widespread arid conditions across the North American Craton during the Meramecian (Mississippian). Therefore, another potential source for

the medium to coarse silt-sized chert grains is eolian dust, sourced from arid landmasses upwind of the deeper-water Tobosa Basin (Cecil, 2004).

Burrows in the mudstones are generally horizontal, and *Chondrites* and *Zoophycos* are present in several intervals. Total organic carbon ranges from 1.01 to 1.81%. The moderate levels of TOC and horizontal burrows suggest a dysaerobic environment that had periods of both anoxic and oxic conditions. The mudstones are interpreted to be deeper-water deposits on the basin floor. Sediments were probably delivered by a combination of dilute turbidity currents from upslope and pelagic sedimentation from the water column. Infaunal components could have been transported from updip environments and terminated their lives as doomed pioneers in the low oxygen or periodically dysoxic environment.

Argillaceous Skeletal Wackestone to Packstone

Argillaceous skeletal wackestone to packstone (Fig. 11) is found at the base and top of the Two Finger Sand interval. It is commonly intercalated with argillaceous mudstone and burrowed to laminated lime argillaceous siliceous packstone. Allochems are composed of crinoids, brachiopods, spicules, algae, and rare trilobite fragments (Figs. 11A and 11B). Most of the organisms are of a heterozoan assemblage. They are fragmented and highly abraded.

This facies occurs as 2 to 6 mm thick discrete laminations that amalgamate and have thicknesses of up to 1 ft (~0.3 m). Flow types range from cohesive flows with large allochems floating in the matrix to noncohesive flows that display internal sorting and grading (Fig. 11C). Lithofacies range from matrix supported (common) (Fig. 11D) to bioclast supported (uncommon) (Fig. 11B). The matrix is composed of subequal amounts of clay and silt and is commonly chaotically organized. The allochems
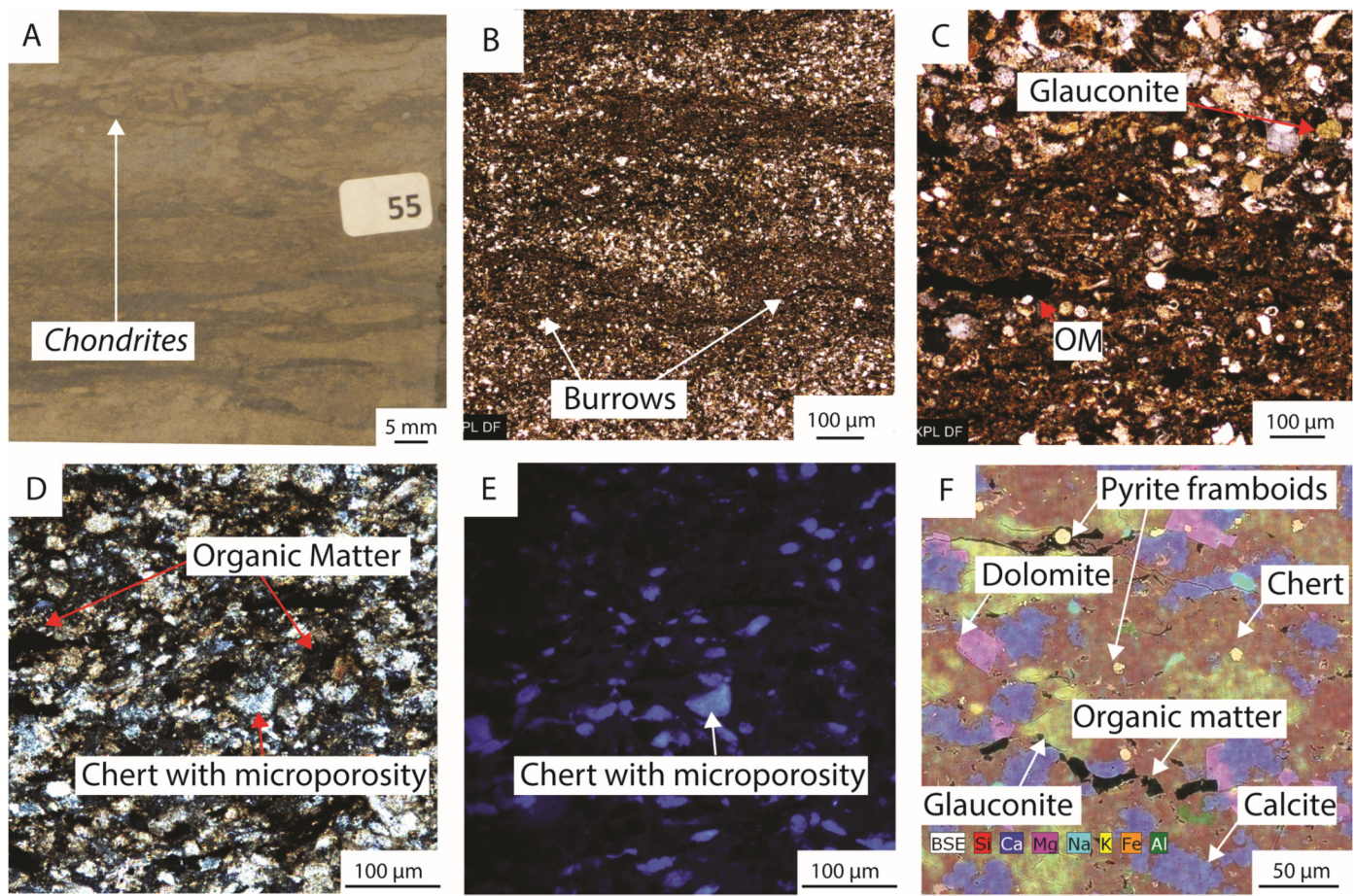
Figure 8. Photographs of burrowed to laminated lime argillaceous siliceous packstone lithofacies. (A) Core photograph showing burrows obscuring original sedimentary features. Lower Two Finger Sand: Anschutz Fasken E11–11, 11,508 ft (~3507 m). (B) Horizontal burrows infilled with a fine-grained matrix. Lower Two Finger Sand: Anschutz Fasken E11–11, 11,500 ft (~3505 m). (C) Detailed fabric of burrow and surrounding lithology; glauconite, peloids, and shell fragments are common. Lower Two Finger Sand: Anschutz Fasken E11–11, 11,500 ft (~3505 m). (D) Abundant chert grains with micropores. Lower Two Finger Sand: Anschutz Casselman 14–10, 11,540 ft (~3517 m). (E) Same image as D but under UV light that emphasizes micropores. Lower Two Finger Sand: Anschutz Casselman 14–10, 11,540 ft (~3517 m). (F) EDS mineralogical map of the burrowed lime argillaceous siliceous packstone lithofacies. Lower Two Finger Sand: Anschutz Fasken 215B, 11,525.1 ft (~3512 m).

are silt to cobble sized and are generally not well sorted. This facies contains subangular to subrounded phosphatized allochems and phosphatized intraclasts (Fig. 11D).

According to EDS point counting, calcite comprises 28.5%, clay 44.5%, and quartz 15%. Minor amounts of dolomite (2%) and pyrite (2.6%) are present. TOC ranges from 1 to 1.2%. Identified kerogen types range from type III woody macerals to type II algal macerals (Fig. 11E).

Skeletal Grainstone

Skeletal grainstone (Fig. 12) is found only in the Exxon Fasken Block B No. 1 well, which is located in a more proximal location (Fig. 3). Individual bed thicknesses range from <1 ft (~0.30 m) to 5 ft (~1.5 m). The fabric is massive bedded and displays no internal organization (Figs. 12A–12F). Textural components in this lithofacies are oolitic coated grains that are extensively micritized and are commonly nucleated on quartz grains (Figs. 12D–12F), bivalves, and echinoderm plates. These are interpreted as noncohesive massive-bedded turbidite units.

The ooid-coated grains that characterize this lithofacies are moderately sorted and well rounded, with poor to moderate sphericity. Pore space is almost completely occluded with calcite and dolomite cements. Porosity values range from 0.4 to 1.7% and

permeability is not measurable using standard permeability analysis. According to thin-section point counting, mineralogy of this lithofacies is primarily calcite (>90%) and quartz (<10%).

STRATIGRAPHIC ARCHITECTURE

The Two Finger Sand interval in the Barnett Formation is interpreted to have been deposited in a deepwater, carbonate-fan complex (Candelaria, 1990; Osterlund, 2012; Entzminger, 2015). Deepwater carbonate slopes and basins contain both fine-grained hemipelagic sediments and fine- to coarse-grained gravity-flow deposits. The main difference between the slope and basinal sediments is that the slope and base-of-slope sediments are more commonly disrupted and chaotically deformed, while basinal sediments are usually finer textured and occur in organized upward-fining sequences (Cook and Mullins, 1983). Submarine fans commonly include slope, inner-fan, middle-fan, and outer-fan systems (Fig. 13) (Cook and Mullins, 1983). In the study area, the Two Finger Sand interval submarine fan includes basinplain (argillaceous mudrock) and fan-fringe deposits (thinlybedded turbidites and hybrid-event beds). Distal portions of deepwater fans are commonly composed of hybrid sediment gravity flows (Haughton et al., 2009). The Two Finger Sand interval hybrid-event bed units contain H1, H2, H3, H4, and H5
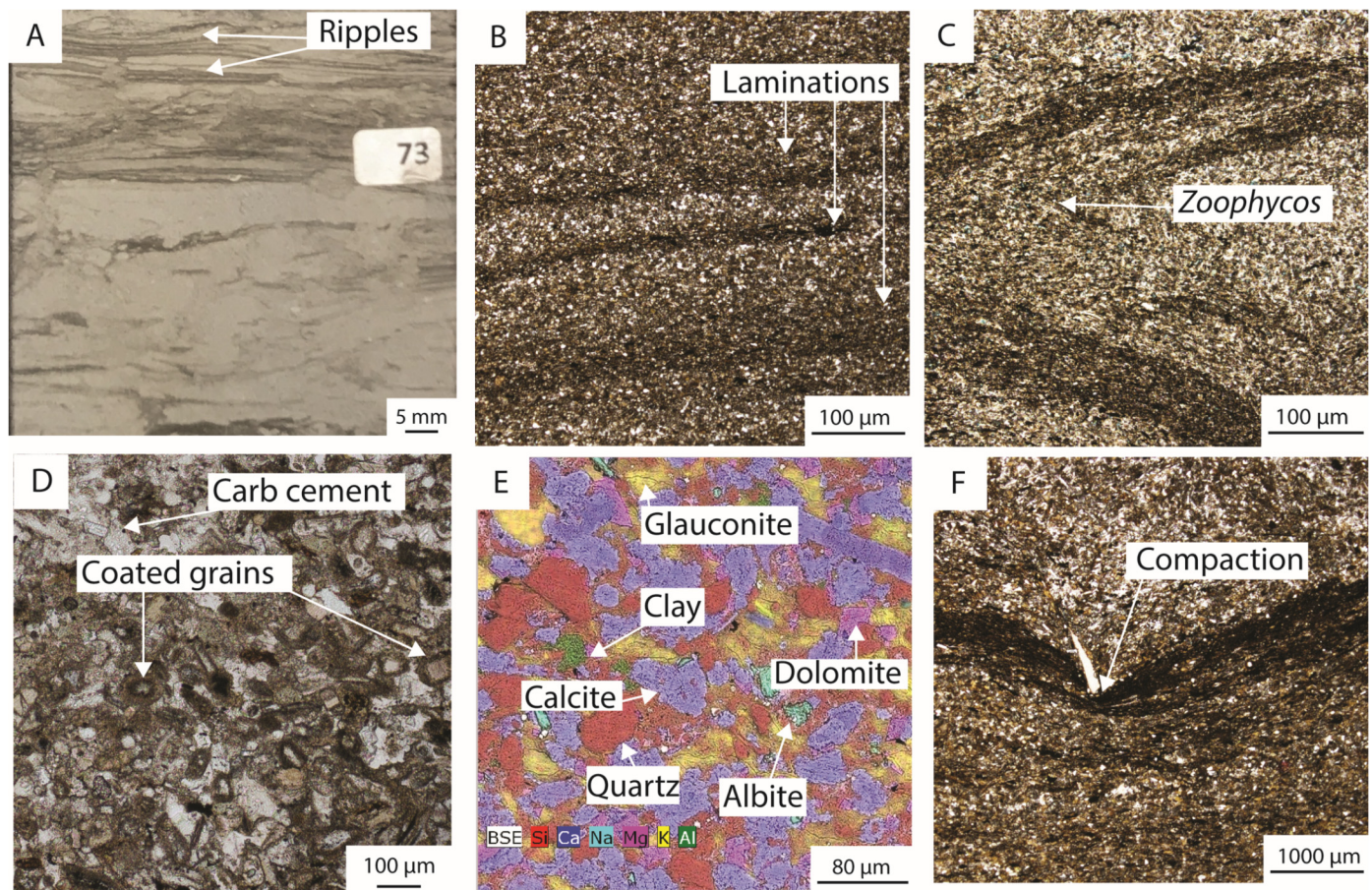
Figure 9. Photographs of burrowed to laminated siliceous lime packstone lithofacies. (A) Core photograph showing an upward-fining sequence capped with ripple laminations. Upper Two Finger Sand: Exxon Fasken Block B No. 1, 11,630 ft (~3544 m). **(B)** Event beds arranged in 0.5–1.25 mm upward-fining laminae. Lower Two Finger Sand: Anschutz Fasken 6–13, 11,507 ft (~3507 m). **(C)** *Zoophycos* burrow. Lower Two Finger Sand: Exxon Fasken Block B No. 1, 11,661 (~3554 m). **(D)** Grainstone with coated grains and shell fragments with calcite cement occluding porosity. Lower Two Finger Sand: Exxon Fasken Block B No. 1, plane-polarized light, 11,646 ft (~3550 m). **(E)** SEM–based EDS mineralogy of burrowed to laminated siliceous lime packstone: rare clay minerals, abundant carbonate and quartz grains, and minor ferroan dolomite and albite grains. Lower Two Finger Sand: Anschutz Fasken 6–13, 11,509 ft (~3507 m). **(F)** Compaction of fine-grained laminae around skeletal debris. Lower Two Finger Sand: Anschutz Fasken 6–13, 11,517 ft (~3510 m).

divisions of hybrid-events beds (Figs.14A–14C). Hybrid-event bed thicknesses range from <0.02 in to 3 ft (~0.5 mm to 1 m).

The ideal hybrid-event bed in the Two Finer Sand interval (Fig. 14B), from the base to the top, consists of the following: (1) H1: clay-poor lime packstone with silt- to sand-sized carbonate and siliceous fragments that is commonly structureless and contains isolated mudclasts and organic matter; (2) H2: banded lime packstone with alternating light and dark units, concentrated carbonaceous seams, and water-escape features; (3) H3: silty mudstone with common skeletal-rich layers, sand-injection features, clay clasts, and contorted layers; (4) H4: lime packstone with ripples, that have been highly disrupted by burrows, and parallel laminations that are dilute turbidity currents with a prevalence of type III organic matter that accumulated towards the top of the laminations; and (5) H5: thin-bedded and argillaceous mudstone that is a product of suspension settling of the finer fraction of turbidity plumes.

Lower Two Finger Sand Unit

The lateral dimensions of the Lower Two Finger Sand unit—approximately 25 mi (~40 km) in the north to south direction by 35 mi (~56 km) in the east to west direction—comprises an areal extent roughly 650 sq mi (~1680 sq km) (Fig. 15). The Lower Two Finger Sand unit displays a fan sheet-like geometry with an average thickness of 35 ft (~10.7 m). Along the northern inner-ramp, the Lower Two Finger Sand unit achieves a thickness of 30 ft (~9.14 m). In the depocenter, the Lower Two Finger Sand unit reaches a maximum thickness of 60 ft (~18.3 m). At this point there is a bifurcation of the fan lobes, with the western lobe oriented perpendicular to the northern inner ramp and the eastern lobe slightly oblique to the northern inner ramp. Near the fan terminus, the Lower Two Finger Sand unit is approximately 15 to 25 ft (~4.5 to 7.6 m) thick and rapidly thins to the south. Sediment supply appears to have been from the northern and eastern inner-ramp, coalescing into a multitude of fan lobes in the basin. Because of widespread erosion from the uplift of the Central Basin Platform, another potential sediment-source direction was from the western margins of the basin. However, because much of the Mississippian section was removed by erosion during the Late Mississippian to Late Pennsylvanian (Frenzel et al., 1988; Hamilton and Asquith, 2000), correlations are not possible.

Upper Two Finger Sand Unit

The lateral dimensions of the Upper Two Finger Sand unit—approximately 25 mi (~40 km) in the north to south direction by
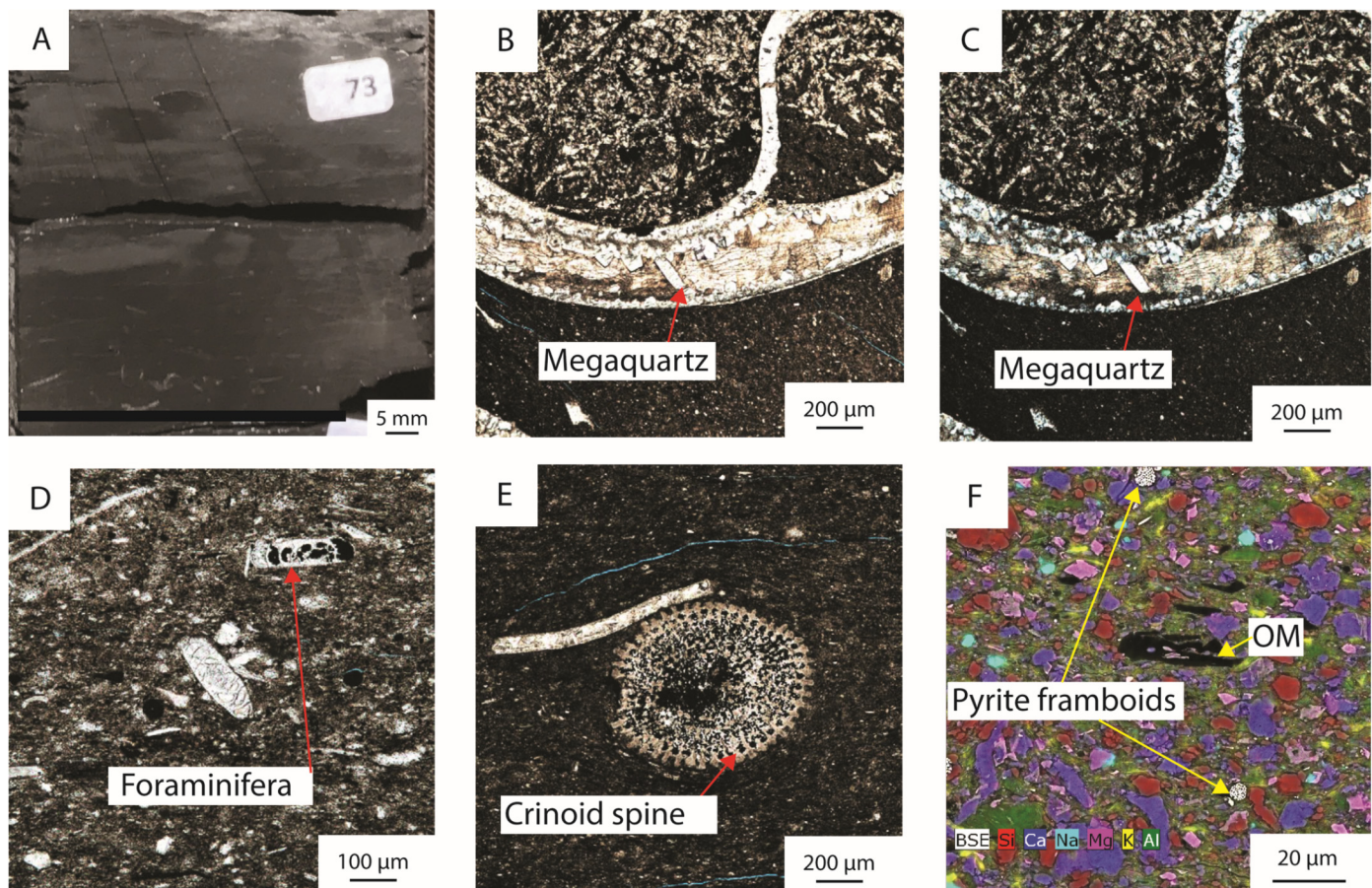
Figure 10. Photographs of argillaceous mudstone lithofacies. (A) Core photograph of structureless argillaceous mudstone (surface wetted). Lower Two Finger Sand: Anschutz Casselman 14–10, 11,516 ft (~3507 m). (B) Brachiopod with megaquartz silicification. Lower Two Finger Sand: Anschutz Casselman 14–10, 11,510 ft (~3505 m). (C) Same image as B, but under cross-polarized light. Lower Two Finger Sand: Anschutz Casselman 14–10, 11,516 ft (~3507 m). (D) Foraminifera with euhedral pyrite replacement. Lower Two Finger Sand: Anschutz Casselman 14–10, 11,514 ft (~3509 m). (E) Crinoid spine with euhedral pyrite replacement. Lower Two Finger Sand: Anschutz Fasken 215B, 11,546 ft (~3519 m). (F) EDS mineralogy showing clay matrix and silt-sized particles of carbonate, quartz, dolomite, and albite. Lower Two Finger Sand: Anschutz Fasken 215B, 11,546 ft (~3519 m).

30 mi (~48 km) in the east to west direction—comprises an areal extent of 600 mi² (~1550 km²) (Fig. 16). The areal extent of the thickest portion of the Upper Two Finger Sand unit (40 to 60 ft [~12 to 18 m]) is only 160 sq mi (~415 sq km), in contrast to the Lower Two Finger Sand unit, which has a much more consistent thickness throughout the study area. The Upper Two Finger Sand unit depositional lobes display compensational stacking in the northern area where the Lower Two Finger Sand unit is the thin. Along the northern and eastern inner-ramp, the Upper Two Finger Sand unit has a thickness of 30 ft (~9.14 m). The log pattern of this unit basinward of the inner-ramp is an upward-coarsening gamma-ray log signature with a gradational base (Fig. 13). To the south, the unit thickens to a maximum of 60 ft (~18.3 m) and then rapidly thins to zero in approximately 10 mi (~16 km) in northern Midland County.

Stratigraphic Architecture Based on Wireline-Log Corrections

Cross section A–A' (Fig. 17) displays a maximum topographic variation of approximately 250 to 300 ft (~76–91 m) from the northern inner-ramp to the distal reaches of the fan complex, assuming that the Strawn datum approximates the original depositional profile. Cross section A–A' shows potential sediment-source areas from the northern area of the carbonate ramp.

Proximal to the inner-ramp are thin upward-fining log signatures (inverted funnel-shaped gamma-ray log response), interpreted as slope channels that allowed sediment bypass of shallow-water inner- and middle-ramp components to be transported to the fan by turbidity-current and debris-flow processes (Fig. 13). In the study area, the Two Finger Sand interval display two upward-coarsening gamma-ray-log signatures (funnel-shaped gamma-ray log response) (Candelaria, 1990) that are interpreted as depositional lobes along the fringe of a fan complex (Figs. 2 and 11). Gamma-ray log signatures abruptly transition upward into a gamma-ray log signature with high gamma-ray values that are interpreted as a clay-rich basinal units.

DEPOSITIONAL MODEL

On the basis of sedimentary structures, lithofacies, and trace fossils, a depositional model was constructed that accounts for the depositional processes and products observed in the Two Finger Sand interval (Fig. 18). The Two Finger Sand interval depositional facies in the Tobosa Basin are interpreted to have formed below storm-wave base in an outer-ramp to basinal setting in estimated water depths of 300 to 750 ft (~90 to 230 m). The sediments were deposited in a dysaerobic to anoxic basin that had brief periods of oxygenation. Deposition of the fan units was dominated by hybrid-event beds that contained both
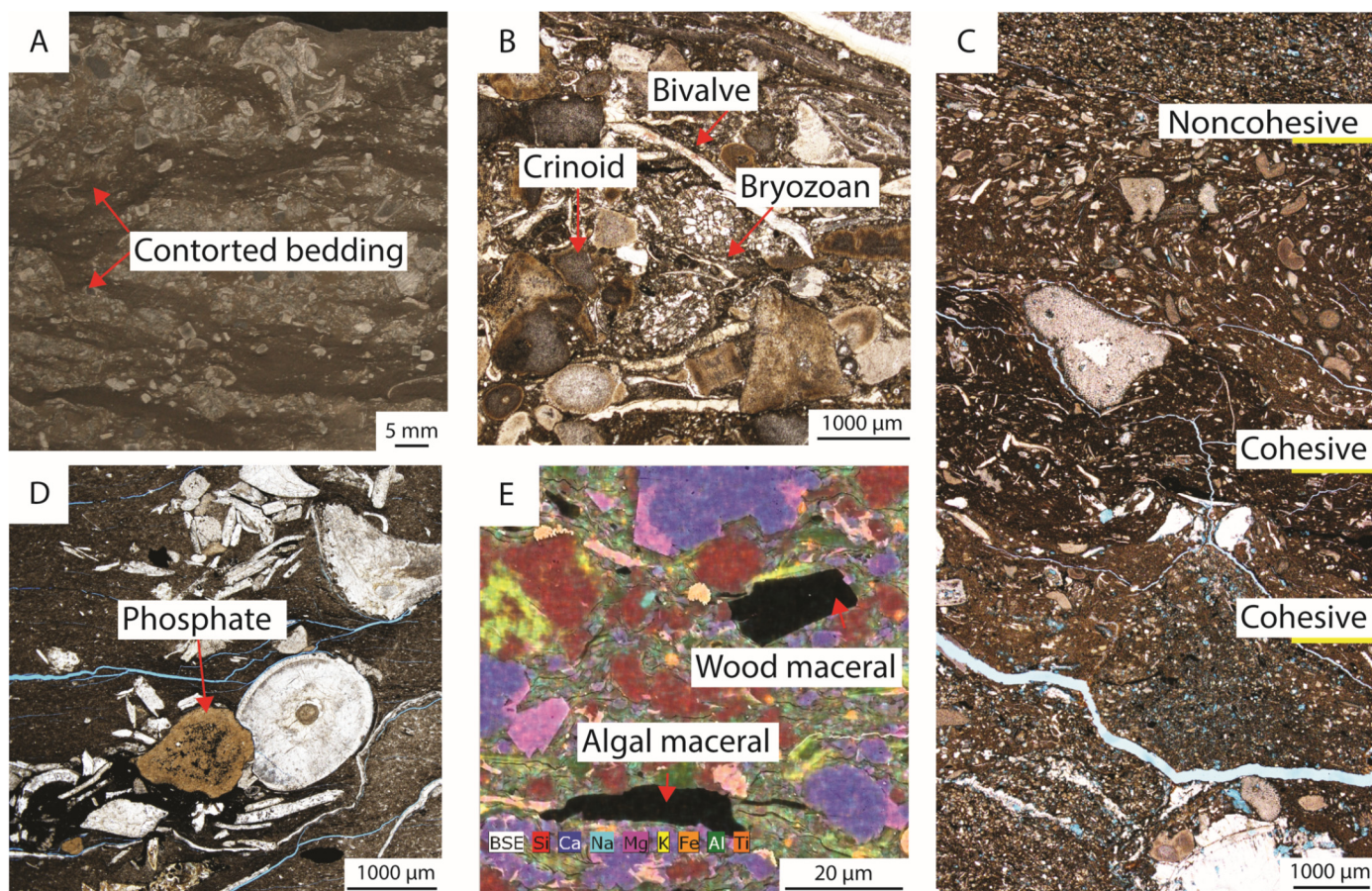
Figure 11. Photographs of argillaceous skeletal wackestone to packstone lithofacies. (A) Core photograph of contorted layers in a cohesive mud matrix. Upper Two Finger Sand: Anschutz Fasken 215B, 11,485.5 ft (~3500 m). (B) Abundant bryozoan fragments and concentrated crinoid and bivalve grains. Upper Two Finger Sand: Exxon Fasken Block B No. 1, 11,638 ft (~3547 m). (C) Vertical succession through a debris flow showing layering (tops of flow events highlighted in yellow). Both normal and inverse grading occurs. Unit displays both cohesive and noncohesive matrix. Lower Two Finger Sand: Anschutz Fasken E11–11, 11,490 ft (~3502 m). (D) Phosphate intraclast, crinoids, brachiopods, and bivalve shells in clay to silt matrix. Upper Two Finger Sand: Anschutz Fasken 215B, 11,452 ft (~3490 m). (E) SEM–based EDS mineralogy showing clay, calcite, dolomite, quartz and organic matter. Organic fraction contains wood and algal macerals. Lower Two Finger Sand: Anschutz Fasken E11–11, 11,490 ft (~3502 m).

cohesive and noncohesive cogenetic flows (Mulder and Alexander, 2001; Haughton et al., 2009). Suspension settling of the pelagic fraction (laminations) and dilute turbidity currents and bottom-current reworking (starved ripples, minor scour surfaces, and laminations) are responsible for the observed sedimentary structures (Fig. 19). The calcareous fraction (grains, brachiopods, and echinoderm plates) in the packstone units is interpreted as allodapic material from the proximal ramp (inner and middle). The only deepwater faunal components observed are cephalopods and radiolarians.

Initiation mechanisms of the event beds are commonly caused by liquefaction (Iverson, 1997) that is associated with seismic activity and storm-wave loading (Chen and Lee, 2013). Other potential sediment-delivery mechanisms include storm-return flow (Dyson, 1995), slope failure (Yurewicz, 1977), and over-steepened mud mounds (Dorobek and Bachtel, 2001). In the Mississippian strata from the Sacramento and San Andres Mountains, Bachtel and Dorobek (1998) provided evidence of slope readjustment in a progressively steepening carbonate-ramp setting. Calciturbidites were delivered to the deep basin from sediments produced by submarine erosion into underlying strata during lowstand-systems-tracts episodes. Similar submarine erosional surfaces may have created sediment-bypass conduits

that persisted throughout the ensuing time periods and allowed delivery of the Two Finger Sand interval sediments to the basin.

ORGANIC-MATTER ANALYSIS

Samples were mainly selected from the darker argillaceous mudstones, but some were taken from the carbonate/siliceous packstone and the argillaceous skeletal wackestone to packstone lithofacies. TOC values range from 0.62 to 3.1% (Fig. 20), with the average value being 1.40%. T_{max} (heat index of organic matter) values range from 448 to 465ºC, with an average value of 454ºC. Based on T_{max}, R_o values were calculated (average 1.12% and range from 0.9 to 1.21%). TOC values are relatively consistent with those reported by Candelaria (1990), who published TOC values ranging from 1.1 to 4.7%, but R_o values are much lower than his average of 1.47% in the neighboring Desperado Field (Fig. 3). This situates the Two Finger Sand interval in the Moonlight Field (Fig. 3) in the late oil to early gas window. Fair to excellent TOC values suggest that the sediments must have been deposited in dysaerobic to anaerobic bottom waters to have been preserved.

Type III organic matter was the primary kerogen type observed based on Rock-Eval® analysis, as well as the size and
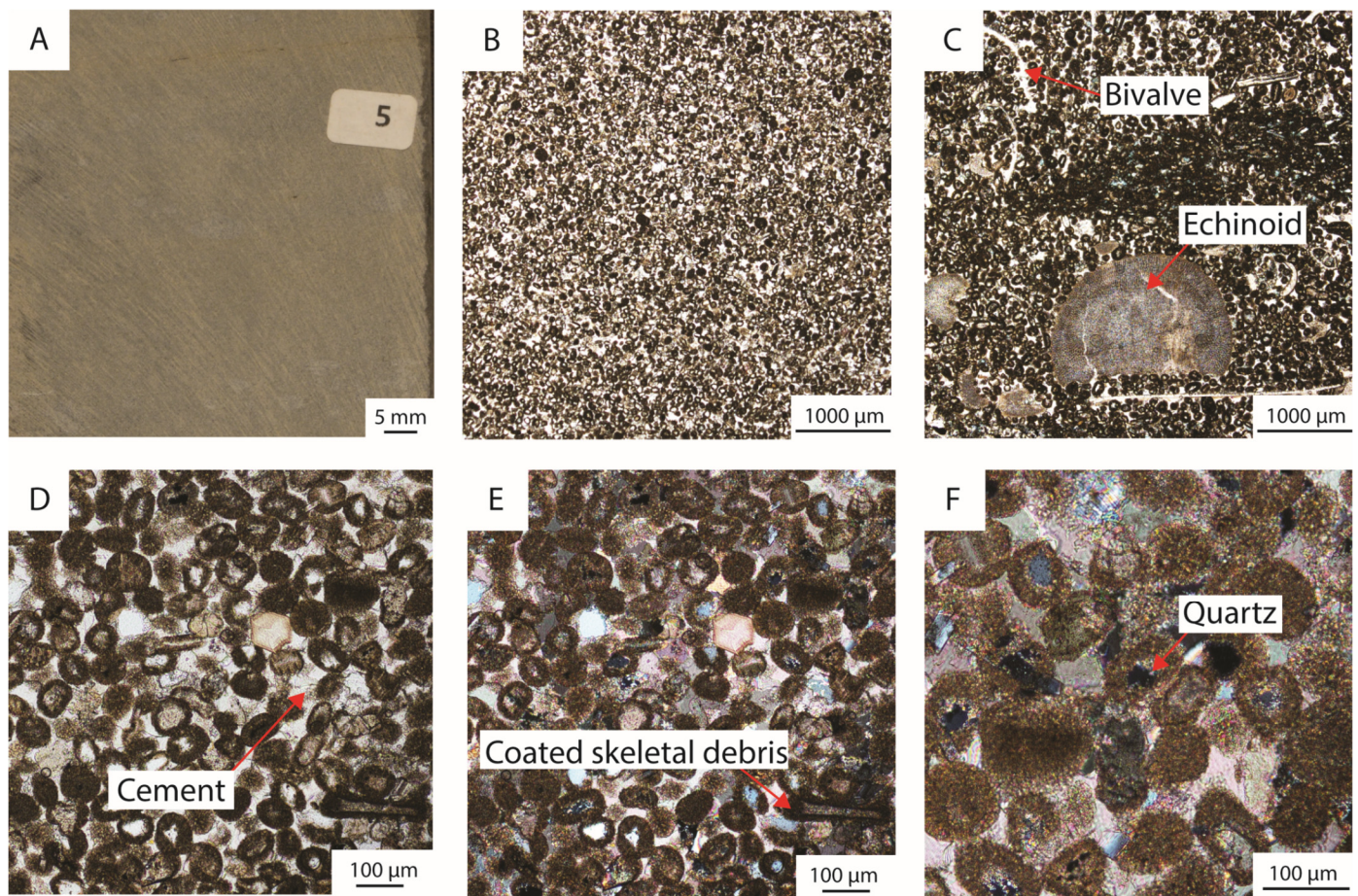
Figure 12. Photographs of skeletal grainstone lithofacies. (A) Skeletal grainstone lithofacies showing massive bedding. Upper Two Finger Sand: Exxon Fasken Block B No. 1, 11,612 ft (~3539 m). (B) Texture of skeletal grainstone. Upper Two Finger Sand: Exxon Fasken Block B No. 1, 11,601 ft (~3535 m). (C) Ooid-coated grains, echinoids, and bivalve fragments are the primary components. Upper Two Finger Sand: Exxon Fasken Block B No. 1, 11,628 ft (~3544 m). (D) Ooid-coated grains cemented by calcite. Upper Two Finger Sand: Block B No. 1, 11,601 ft (~3535 m). (E) Same image as D, but under cross-polarized light. Upper Two Finger Sand: Exxon Fasken Block B No. 1, 11,601 ft (~3535 m). (F) Close-up of coated grains with quartz-grain nuclei. Upper Two Finger Sand: Exxon Fasken Block B No. 1, 11,601 ft (~3535 m).

morphology of the organic-matter particles (Fig. 21A). The particles are composed of larger macerals (>10 µm) that appear relatively rigid and uncompacted. Most of the type III organic matter in the Two Finger Sand interval has no organic-matter pores (Fig. 21B), although a few particles do contain inherited pores (Fig. 21C) (Loucks and Reed, 2014; Reed and Ruppel, 2014). Rare type II organic matter occurs in the argillaceous mudrock (Fig. 21D) that may be a ripped-up bacterial mat not uncommon in anoxic settings (Gorin et al., 2009). The mat shows inclusion of pyrite and calcite grains (<5 µm). Type II organic matter commonly has well-developed organic-matter porosity at the observed maturity values (Loucks et al., 2009; Loucks et al., 2012; Loucks and Reed, 2014), but no nanopores were observed in this example.

Rock-Eval® data (pyrolysis peak values S1 + S2 versus TOC) grainstones were not sampled). The Two Finger Sand interval has generally good TOC values but generally poor generative potential (S1 + S2). The facies with the widest range of TOC and generative potential is the burrowed to laminated lime argillaceous siliceous packstone. Hybridized debris flows commonly have a concentration of terrigenous organic matter toward the tops of units similar to what Haughton et al. (2009) observed. Higher TOC values are consistently observed in the tops of siliceous packstone packages, within the H3 division, that are lami-

nated and contain no burrows in the Two Finger Sand interval coarser units. Therefore, the tops of packstone units just before lobe switching contain the highest TOC values.

RESERVOIR QUALITY

The Moonlight Field (Fig. 3) has produced 1,300,676 barrels (bbls.) (~206,790 m³) of condensate, 3.32 billion cubic ft (Bcf) (~94 million m³) of gas, and 41,844 bbls (~6652 m³) of water from the Lower Two Finger Sand unit. Only 1 year after discovery, the Moonlight Field had already produced 729,000 bbls of oil (Pausé et al., 1985). The produced condensate is high American Petroleum Institute (API) gravity (60–70°) and contains a gas to oil ratio of 3000 to 1 (Candelaria, 1990). All of the wells in the Moonlight Field are overpressured, with high pressure gradients of 0.7 psi/ft (~0.16 MPa/m) and initial reservoir pressures of 7500 to 10,000 psi (~52 to 69 MPa) (Candelaria, 1990). Older vertical wells were generally completed with 60,000 to 70,000 gallons (~227,000 to 265,000 l) to of diesel or lease crude and 50,000 to 100,000 lb (22,700 to 45,400 kg) of sand proppant (Candelaria, 1990).

The Two Finger Sand interval contains low porosity values (0.5 to 7.5%) and very low permeability values (<0.001–0.06 md) based on core-plug analyses. The lowest porosity values

Figure 13. Carbonate submarine fan model showing the vertical succession of facies sequences that occur in the Tobosa Basin during the Late Mississippian (slightly modified after Cook and Egbert, 1981; Cook and Mullins, 1983). (1) Mabee Ranch 318–1 showing a vertical succession composed of upward-fining distributary channels, blocky lobe sheets, and upward-fining feeder channels. (2) Mabee JE A NCT 1–261 showing a vertical succession composed of thinly-bedded hybrid-event beds, blocky lobe sheets, and upward-fining distributary channels. (3) Getty-Fasken 1–19 showing a vertical succession of basin plain deposits, dilute turbidity currents, and thinly-bedded hybrid-event beds.
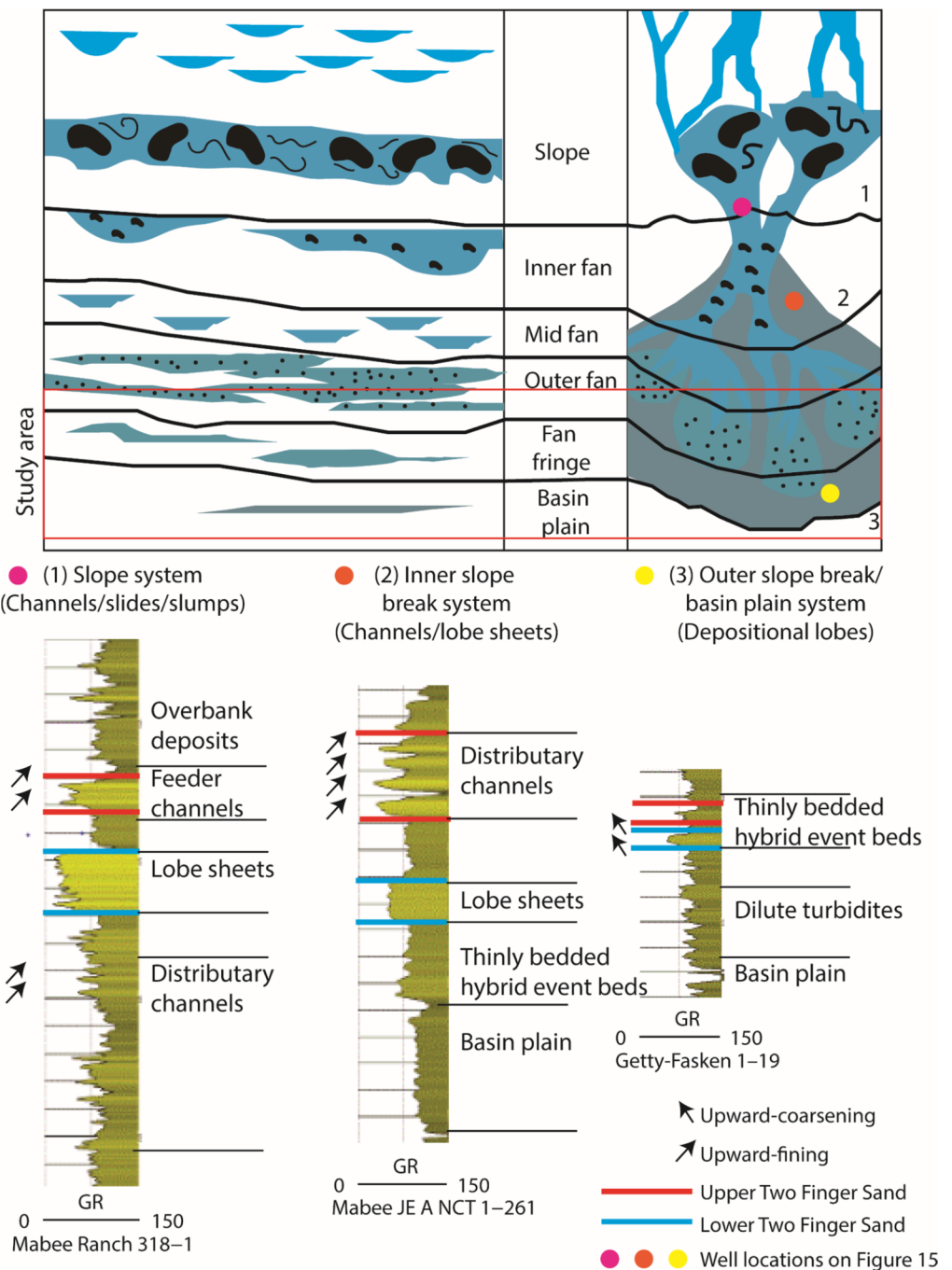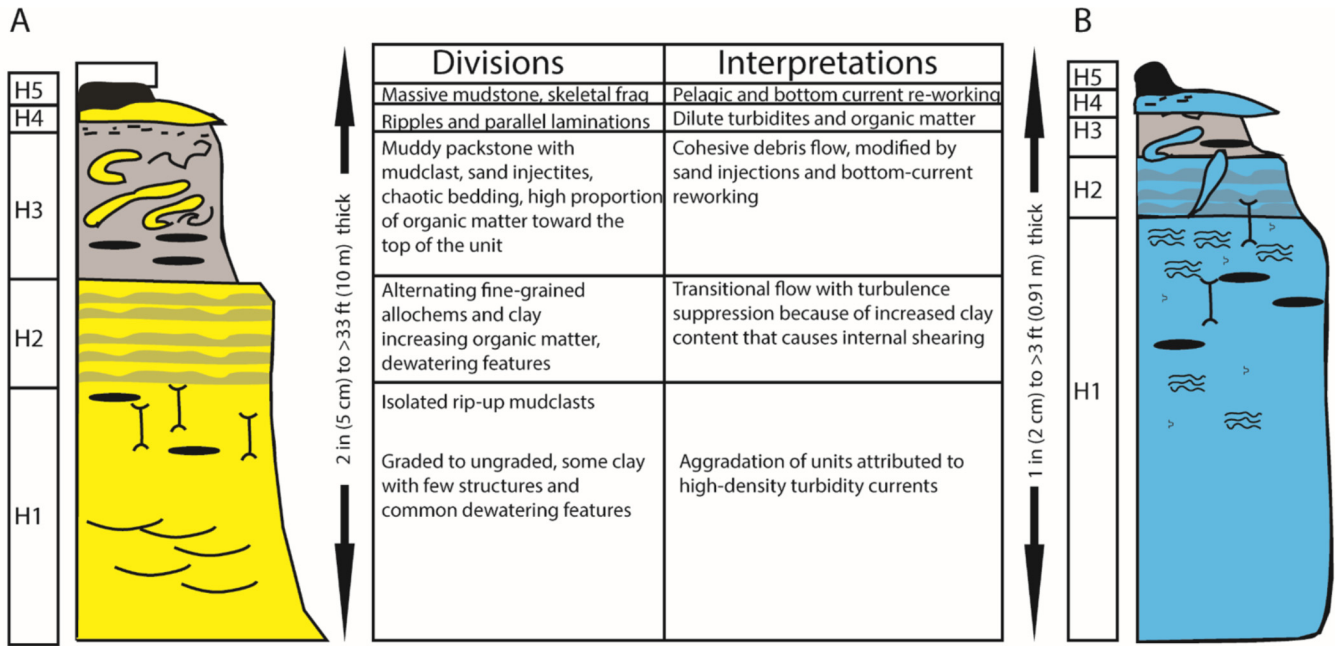

(**FACING PAGE**) **Figure 14. Hybrid-event beds. (A) Idealized divisions of hybrid-event beds (slightly modified after Haughton et al., 2009). (B) Idealized divisions of the Two Finger Sand hybrid-event beds. (C) Core photographs of the hybrid-event bed divisions found within the Two Finger Sand. (H5) Discrete ripples in a massive mud matrix that are likely the result of bottom-current reworking. (H4) Packstone with ripples towards the top of the sand unit. (H3) Mudstone with contorted argillaceous skeletal wackestone to packstone. (H2) Banded lime packstone with water-escape feature and alternating light and dark layers. (H1) Lime packstone with silt- to sand-sized carbonate grains and siliceous skeletal fragments, mudclasts, and coffee-ground organic matter.**

were observed in skeletal grainstones (average 1.0%) in the Exxon Fasken Block B No. 1 core. Interparticle pores are occluded with calcite cement (Figs. 12D–12F). The burrowed to laminated siliceous lime packstone contains average porosity values of 2.1%. The highest porosity values (average 7.5%) observed are found within the burrowed to laminated lime argillaceous siliceous packstone.

Based on SEM and EDS analyses (Fig. 22), only intraparticle nano- and micropores and very rare organic-matter nano- and micropores were observed. Intraparticle nano- and micropores

A

Divisions	Interpretations
Massive mudstone, skeletal frag	Pelagic and bottom current re-working
Ripples and parallel laminations	Dilute turbidites and organic matter
Muddy packstone with mudclast, sand injectites, chaotic bedding, high proportion of organic matter toward the top of the unit	Cohesive debris flow, modified by sand injections and bottom-current reworking
Alternating fine-grained allochems and clay increasing organic matter, dewatering features	Transitional flow with turbulence suppression because of increased clay content that causes internal shearing
Isolated rip-up mudclasts	
Graded to ungraded, some clay with few structures and common dewatering features	Aggradation of units attributed to high-density turbidity currents

2 in (5 cm) to >33 ft (10 m) thick

B

1 in (2 cm) to >3 ft (0.91 m) thick

⊥ Dewatering structures   ⌐⌐ Sand injectite   ⬬ Clay clasts   ⌒ Dish structures   ≋ Coffee-ground organics

C

H5   Discrete ripples   Massive mud   5 mm

H4   Ripples   73   5 mm

H3   Skeletal debris   5 mm

H2   Alternating light and dark bands   21   Sand injectite   5 mm
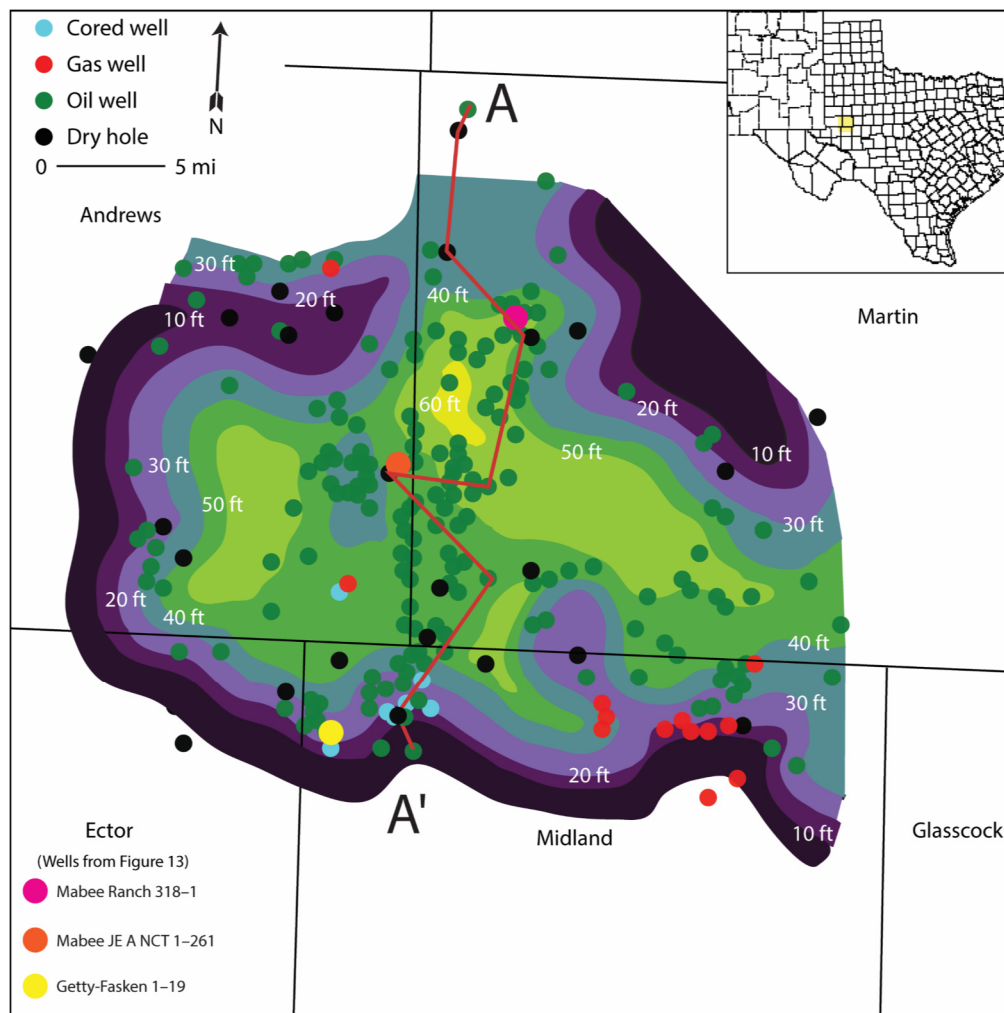
H1   Mudclasts   5 mm
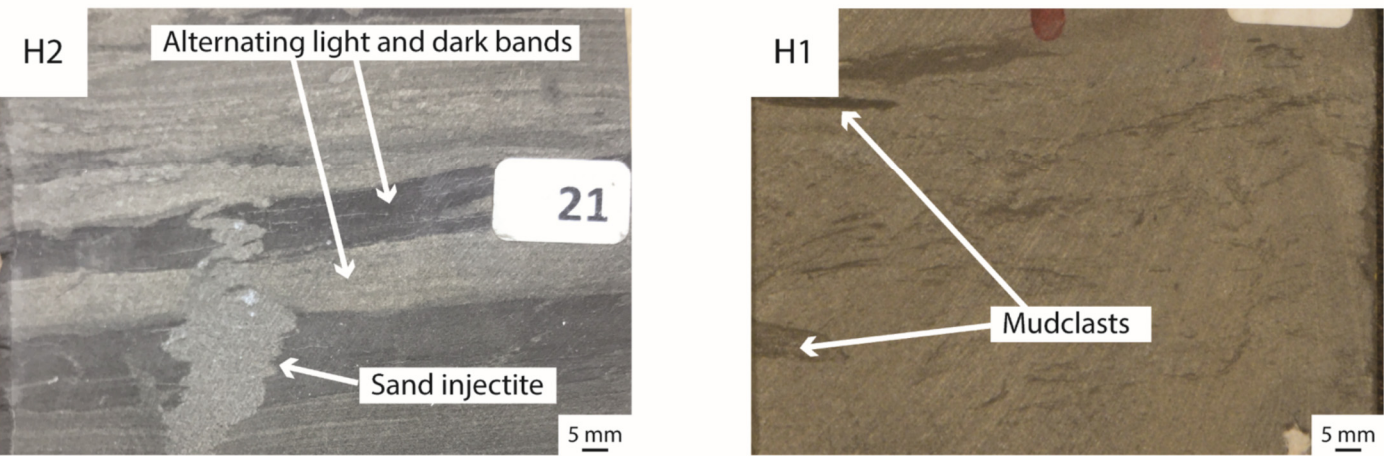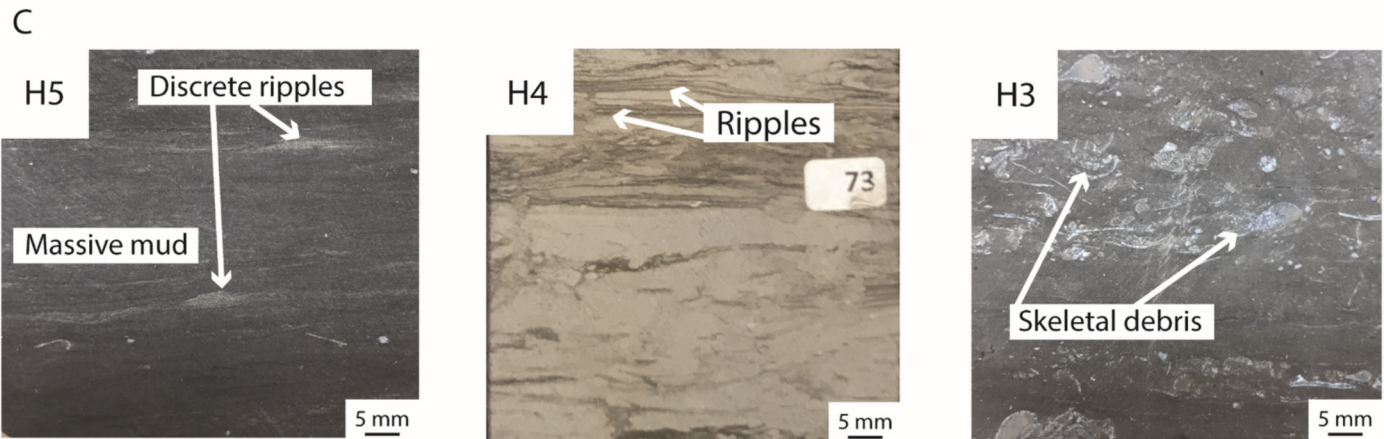
Figure 15. Lower Two Finger Sand unit isopach map. 5 mi = ~8 km.

are present in calcite, clay platelets, quartz, and dolomite grains (Figs. 22A–22D). Intraparticle fluid-inclusion pores occur within the calcite grains (Fig. 22B). These intraparticle fluid-inclusion pores are primarily nanopores; however, some are in the micropore range. Within siliceous grains, larger intraparticle microvugs (5 μm) are developed (Fig. 22C). Some of these microvugs are host to small euhedral quartz crystals. Pyrite grains are also host to intraparticle nanopores (Fig. 22C). Small intraparticle microvugs (4 to 20 μm) within the quartz contain a residual oil coating (Fig. 22D). Unconventional reservoirs with extensive intraparticle nano- and micropores generally have lower permeability values than those with interparticle nano- and micropores (Candelaria, 1990; Loucks et al., 2012).

FRACTURES

Scant evidence exists for fractures in the Moonlight Field cores. Only one vertical calcite-cemented fracture was identified within the studied cores. Because of the extremely low matrix permeability values and lack of apparent well-connected pores, it is postulated that the Two Finger Sand interval's reservoir produced fluids are delivered from a network of natural fractures and, to a lesser extent, the nano- and micropores found within the grains (Candelaria, 1990; this study). Osterlund (2012) also attributes the Two Finger production to natural fractures. Osterlund (2012) stated that abnormal pressure-gradient tests were recorded in the Moonlight Field; a new well was brought online and nearby wells up to 8500 ft (~2590 m) were shut in. The shut-in wells recorded pressure drops within an hour. Such

rapid communication over short distances suggests that an active communicating fracture network is contributing to the reservoir permeability. Additionally, analyzed decline curves are similar to natural-fracture decline curves (Fig. 23) (Blasingame and Lee, 1986). During the first 4 yr of production from the Anschutz Fasken 215B well, the well declined at 40% per yr from fracture production. Throughout the next 27 yr of production, the well produced fluids and gas with only a 3% decline per yr. Following the initial high rates of production, the well was interpreted to have started predominately producing from the low-permeability intraparticle pores (Candelaria, 1990).

CONCLUSIONS

The Two Finger Sand interval is a deepwater submarine fan with an areal extent of approximately 650 mi^2 (1680 km^2) that was deposited in dysaerobic to anaerobic bottom-water conditions. The distal reaches of the coarser-sediment lobes are comprised of <1 in (~2 cm) to <3 ft (~0.9 m) hybrid-event beds that amalgamate vertically and prograde toward the basin center. The submarine fan lobes in the study area are composed of two 15 to 25 ft (~4.5 to 7.6 m) thick sandstone bodies that accumulated in an unconfined setting.

The Two Finger Sand interval contains predominantly type III organic matter that generally generates volatile oil to wet gas. The Two Finger Sand interval exhibits very low porosity values (0.5–7.5%) and extremely low permeability vales (<0.06 md). Only intragranular and very rare organic-matter nano- to micropores were observed. Based on the decline curves and
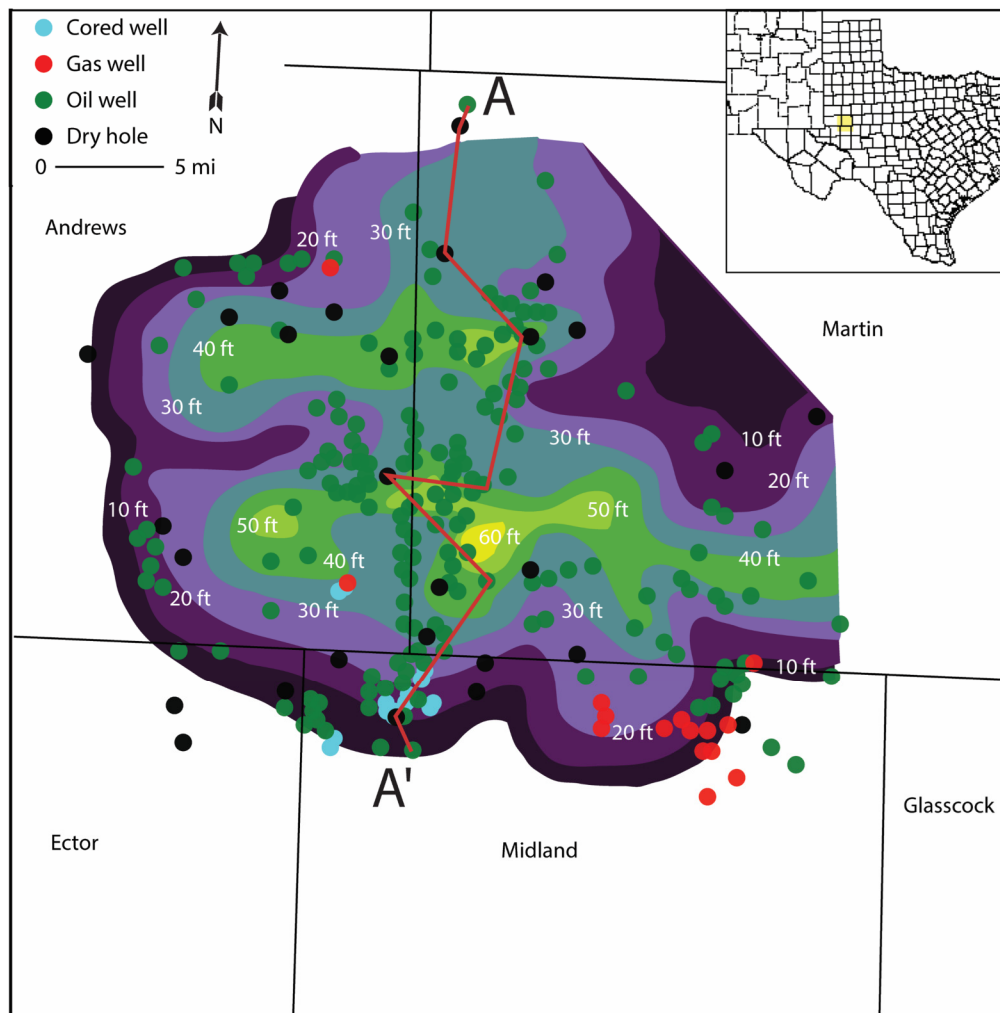
Figure 16. Upper Two Finger Sand unit isopach map. 5 mi = ~8 km.

pressure-gradient tests, it appears that economically successful wells are dominantly a product of a naturally fractured reservoir.

This investigation documented the depositional setting and sediment-source directions of the Two Finger Sand interval. These observations should aid in extending the development of the Two Sand interval or similar units.

ACKNOWLEDGMENTS

REFERENCES CITED

Adams, J. E., 1965, Stratigraphic-tectonic development of the Delaware Basin: American Association of Petroleum Geologists Bulletin, v. 49, p. 2140–2148, <http://archives.datapages.com/data/bulletns/1965-67/images/pg/00490011/2100/21400.pdf> Last accessed February 26, 2018.

Armstrong, A. K., and B. L. Mamet, 1988, Mississippian (Lower Carboniferous) biostratigraphy, facies and microfossils, Pedregosa Basin, southeastern Arizona and southwestern New Mexico: U.S. Geological Survey Bulletin 1826, 40 p., <https://pubs.usgs.gov/bul/1826/report.pdf> Last accessed April 25, 2018.

Bachtel, S. L., and S. L. Dorobek, 1998, Mississippian carbonate ramp-to-basin in south-central New Mexico: Sequence stratigraphic response to progressively steepening outer-ramp profiles: Journal of Sedimentary Research, v. 68, p. 1189–1200, <http://archives.datapages.com/data/sepm/journals/v66-67/data/068/068006/pdfs/1189.pdf> Last accessed February 26, 2018.

Blakey, R., 2005, Paleogeography and geologic evolution of North America; images that track the ancient landscapes of North America: <http://jan.ucc.nau.edu/~rcb7/namM325.jpg> Last accessed February 26, 2018.

Blasingame, T. A., and W. J. Lee, 1986, Properties of homogenous reservoirs, naturally fractured reservoirs, and hydraulically fractures reservoirs from decline curve analysis: Society of Petroleum Engineers Paper 15018, Richardson, Texas, p. 279–294, doi:10.2118/15018-MS.

Broadhead, R. F., 2006, Mississippian strata in southeastern New Mexico, including the Barnett Shale: Thickness, structure and hydrocarbon plays: New Mexico Bureau of Geology and Mineral Resources Open File Report 497, <https://geoinfo.nmt.edu/publications/openfile/downloads/400-499/497/Mississippian%
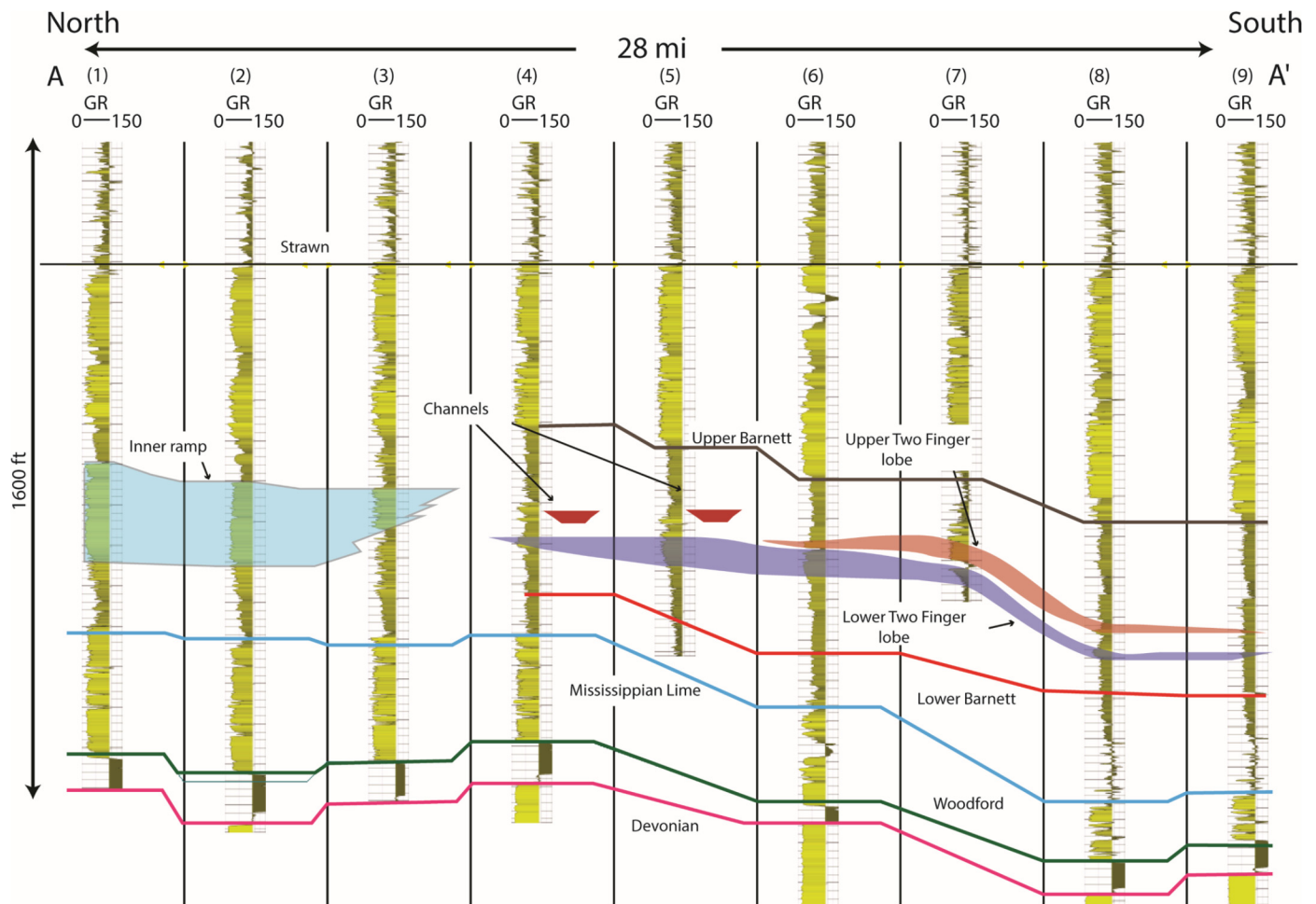
Figure 17. North to south A–A' cross section, datumed on the Strawn Formation. Channels occur close to the inner-ramp (upward-fining log signatures). The lobes are composed of turbidites in the thickest portions of the Two Finger Sand (blocky log signatures with sharp base). At the fringe of the Two Finger Sand lobes, the units are interpreted to be depositional lobes (upward-coarsening gamma-ray wireline log signatures). Wells used in cross section: (1) 42317339260000, Amerind Oil Company University MAK 101; (2) 42317338920000, Amerind Oil Company University 29 1; (3) 42317337600000, BTA Oil Producers 9007 JV–P Block 7 1; (4) 42317345670000, H&M Resources Dorothy Faye 320 1; (5) 42317367030000, Pioneer McReynolds 1; (6) 42003104210000, Texaco JE Mabee A NCT–1 255; (7) 42317377040000, RSP Permian Johnson Ranch 1503; (8) 42329313170000, Exxon Fasken 4015B; (9) 42329311510000, Anschutz Scharbauer 3–27. 28 mi = ~45 km and 1600 ft = ~490 m.

20of%20SE%20New%20Mexico-1.pdf> Last accessed February 26, 2018.

Candelaria, M. P., 1990, "Atoka" detrital a subtle stratigraphic trap in the Midland Basin, *in* J. E. Flis and R. C. Price, eds., Permian Basin oil and gas fields: Innovative ideas in exploration and development: West Texas Geological Society Publication 90–87, Midland, p. 104–106.

Cecil, C. B., 2004, Eolian dust and the origin of sedimentary chert: U.S. Geological Survey Open-File Report 2004–1098, 13 p., <https://pubs.usgs.gov/of/2004/1098/2004-1098.pdf> Last accessed August 18, 2018.

Chen, J., and S. L. Lee, 2013, Soft-sediment deformation structures in Cambrian siliciclastic and carbonate storm deposits (Shandong Province, China): Differential liquefaction and fluidization triggered by storm-wave loading: Sedimentary Geology, v. 288, p. 81–94, doi:10.1016/j.sedgeo.2013.02.001.

Cook, H. E., and R. M. Egbert, 1981, Carbonate submarine fans along a Paleozoic prograding continental margin, western United States (abs.): American Association of Petroleum Geologists Bulletin, v., 65, p. 913, <http://archives.datapages.com/data/bulletns/1980-81/images/pg/00650005/0900/09130.pdf> Last accessed February 26, 2018.

Cook, H. E., and H. T. Mullins, 1983, Basin margin environments, *in* A. P. Scholle, D. G. Bebout, and C. H. Moore, eds., Carbonate depositional environments: American Association of Petroleum Geologists Memoir 33, Tulsa, Oklahoma, p. 540–617, doi:10.1306/M33429.

Craig, L. C., and C. W. Connor, 1979, Paleotectonic investigations of the Mississippian System in the United States: Part I. Introduction and regional analyses of the Mississippian System: U.S. Geological Survey Professional Paper 1010, 369 p., <https://pubs.usgs.gov/pp/1010/report.pdf> Last accessed February 26, 2018.

Dembicki, H., Jr., 2009, Three common source rock evaluation errors made by geologists during prospect or play appraisals: American Association of Petroleum Geologists Bulletin, v. 93, p. 341–356, doi:10.1306/10230808076.

Dorobek, S. L., and S. L. Bachtel, 2001, Supply of allochthonous sediment and its effects on development of mud mounds, Mississippian Lake Valley Formation, Sacramento Mountains, south-central New Mexico, U.S.A.: Journal of Sedimentary Research, v. 71, p. 1003–1016, doi:10.1306/030901711003.

Dyson, I. A., 1995, A review of storm deposits in the geological record: Petroleum Exploration Society of Australia Journal, v. 23, p. 39–50, <http://archives.datapages.com/data/petroleum-
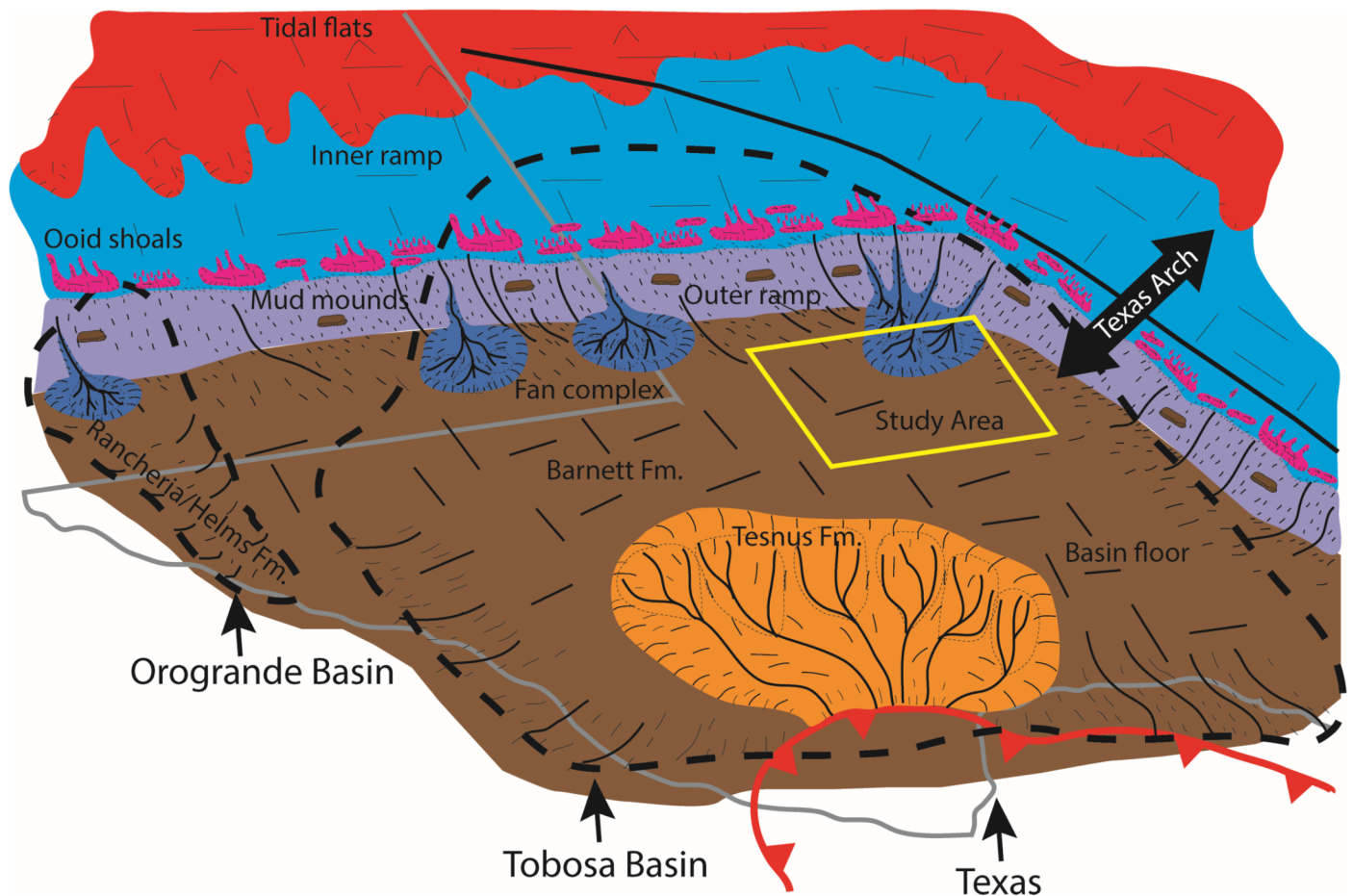
Figure 18. Idealized three-dimensional depositional model in the Tobosa Basin (highly modified after Ruppel and Kane, 2007). Two Finger Sand deposition occurred below storm-wave base in the outer-ramp to basinal setting. Shallow-water components were sourced from updip in the proximal ramp setting.

exploration-society-of-australia/journal/023/023001/pdfs/39. pdf> Last accessed February 26, 2018.

Entzminger, D. J., 2015, Geologic architecture and potential of the Lower Atoka, (Mississippian), Midland Basin: American Association of Petroleum Geologists Search and Discovery Article 9023, Tulsa, Oklahoma, 1 p. <http://www.searchanddiscovery. com/abstracts/pdf/2015/90231playmaker/abstracts/ ndx_entzminger.pdf> Last accessed February 23, 2018.

Ettensohn, F. R., 1993, Possible controls on the origins of extensive ooid-rich carbonate environments, in B. D. Keith and C. W. Zuppann, eds., Mississippian oolites and modern analogs: American Association of Petroleum Geologists Studies in Geology 35, Tulsa, Oklahoma, p. 13–30, <http://archives.datapages. com/data/specpubs/carbona1/images/a048/a0480001/0000/ 00130.pdf> Last accessed February 26, 2018.

Frenzel, H. N., R. R. Bloomer, R. B. Cline, J. M. Cys, J. E. Galley, W. R. Gibson, J. M. Hills, W. E. King, W. R. Seager, F. E. Kottlowski, S. Thompson, III, G. C. Luff, B. T. Pearson, and D. C. Van Siclen, 1988, The Permian Basin region, in L. L. Sloss, ed., The geology of North America, v. D–2: Sedimentary cover—North American Craton; U.S.: Geological Society of America, Boulder, Colorado, p. 261–306, doi:10.1130/DNAG-GNA-D2.261.

Gorin, G., N. Fiet, and M. Pacton, 2009, Benthic microbial mats: A possible major component of organic matter accumulation in the Lower Aptian oceanic anoxic event: *Terra Nova*, v. 21, p. 21–27, doi:10.1111/j.1365-3121.2008.00848.x.

Gutschick, R., and C. Sandberg, 1983, Mississippian continental margins of the conterminous United States, in D. J. Stanley and G. T. Moore, eds., The shelf break: Critical interface on

continental margins: Society of Economic Paleontologists and Mineralogists Special Publication 33, Tulsa, Oklahoma, p. 79–96, <http://archives.datapages.com/data/sepm_sp/SP33/ Mississippian_Continental_Margins.pdf> Last accessed February 26, 2018.

Hamilton, D. C., and G. B. Asquith, 2000, Depositional, diagenetic, and production histories of Chester ooid grainstones in the Austin (Upper Mississippian) Field: Lea County, New Mexico, in W. D. Demis, M. K. Nelis, and R. C. Trentham, eds., The Permian Basin: Proving ground for tomorrow's technologies: West Texas Geological Society Publication 00–109, Midland, p. 95–106.

Haughton, P., P. Davis, W. McCaffrey, and S. Barker, 2009, Hybrid sediment gravity flow deposits—Classification, origin and significance: Marine and Petroleum Geology, v. 26, p.1900–1918, doi:10.1016/j.marpetgeo.2009.02.012.

Iverson, R. M., 1997, Physics of debris flows: Review of Geophysics, v. 35, p. 245–296, doi:10.1029/97RG00426.

Krainer, K., and S. Lucas, 2012, Sedimentary petrography and depositional environments of the type section of the Mississippian Lake Valley Formation, Sierra County New Mexico, in S. Lucas, V. Mclemore, V. Lueth, J. Spielmann, and K. Krainer, Geology of the Warm Springs region: New Mexico Geological Society 63rd Annual Fall Field Conference Guidebook, Socorro, p. 293–304, <http://nmgs.nmt.edu/publications/guidebooks/ downloads/63/63_p0293_p0304.pdf> Last accessed February 26, 2018.

Lane, H. R., 1974, Mississippian of southeastern New Mexico and West Texas—A wedge-on-wedge relation: American Association of Petroleum Geologists Bulletin, v. 58, p. 269–282,
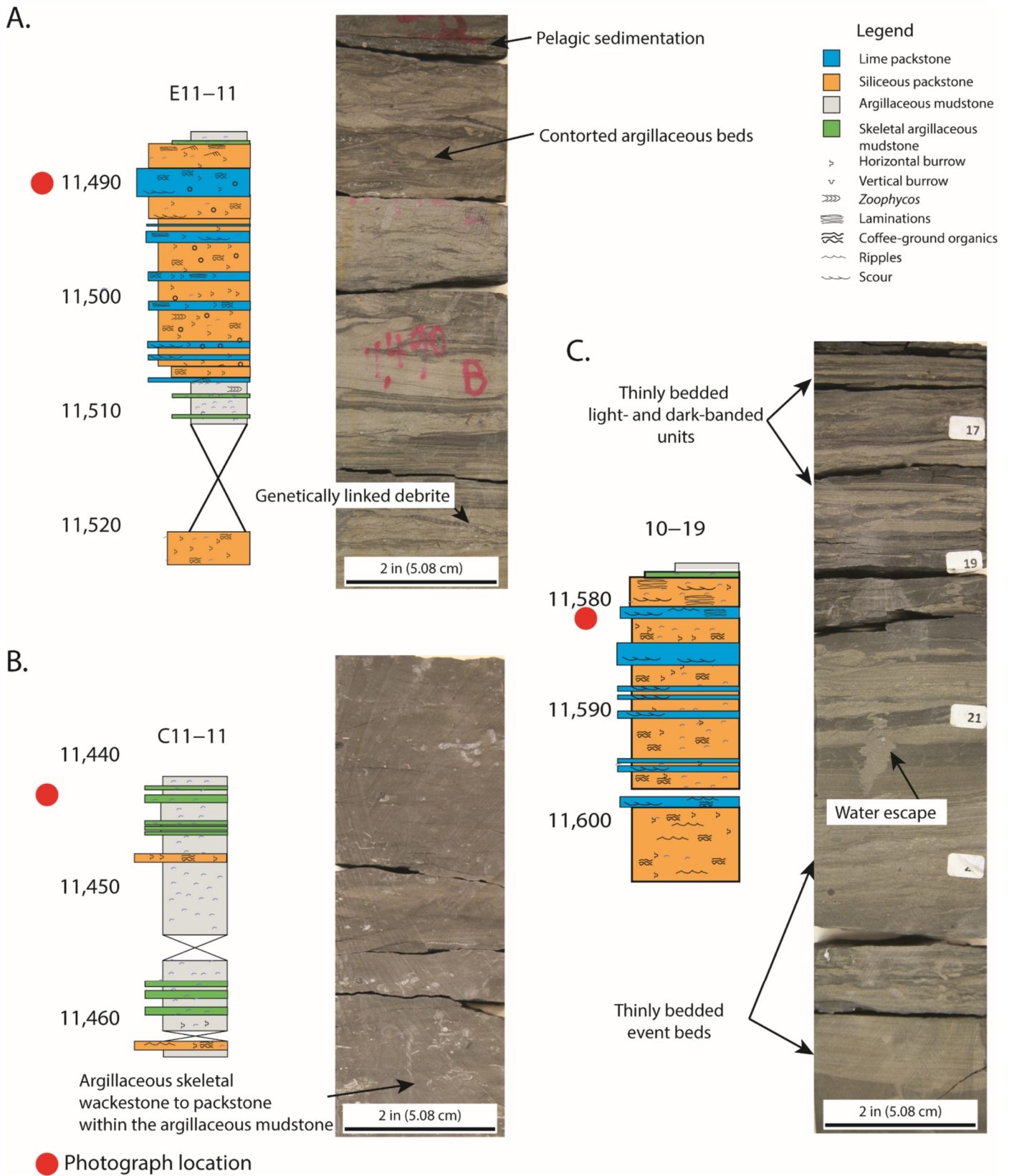
Figure 19. Core description examples with core photographs of sedimentological features. (A) Thinly-bedded carbonate-rich hybrid-event beds with contorted argillaceous layers, capped by pelagic sediments. Lower Two Finger Sand: Anschutz Fasken E11–11, 11,490 ft (~3502 m). (B) Argillaceous mudstone with common, very thinly-bedded argillaceous skeletal wackestone to packstone debris flows. Lower Two Finger Sand: Anschutz C11–11, 11,442 ft (~3487 m). (C) Sequence of hybrid-event bed deposition; carbonate-rich units are capped by thinly-bedded alternating light (traction) and dark (pelagic) units. Lower Two Finger Sand: Anschutz Fasken 10–19, 11,582 ft (~3530 m).
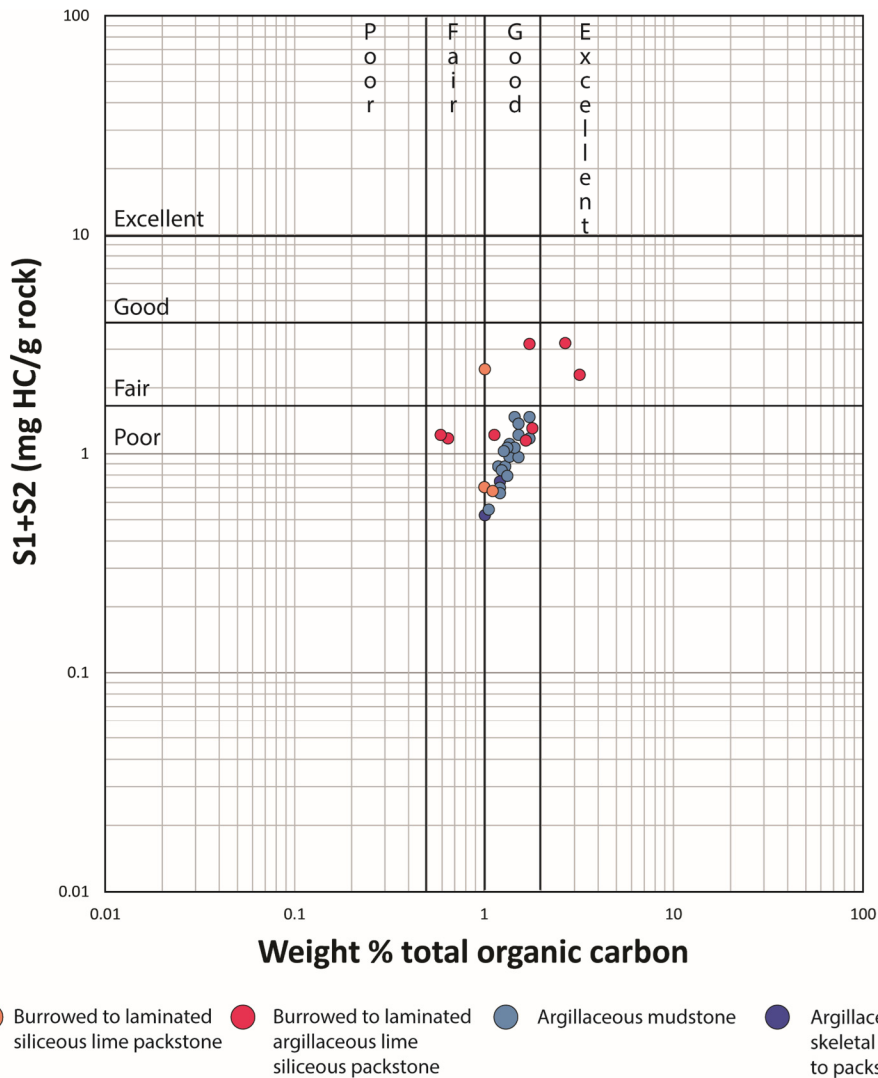
Figure 20. Plot showing the richness and quality of the organic matter. S1 is the measurement of generated hydrocarbons present in sample. S2 is the volume of hydrocarbons that form during pyrolysis of sample. Overall source-rock quality is poor (Dembicki, 2009).

<http://archives.datapages.com/data/bulletns/1974-76/images/pg/00580002/0250/02690.pdf> Last accessed February 26, 2018.

Laudon, L. R., and A. L. Bowsher, 1941, Mississippian formations of the Sacramento Mountains, New Mexico: American Association of Petroleum Geologists Bulletin, v. 25, p. 2107–2160.

Loucks, R. G., and R. M. Reed, 2014, Scanning-electron petrographic evidence for distinguishing organic-matter pores associated with depositional organic matter versus migrated organic matter in mudrocks: Gulf Coast Association of Geological Societies Journal, v. 3, p. 51–60, <http://gcags.org/Journal/2014.GCAGS.Journal/GCAGS.Journal.2014.vol3.p51-60.Loucks.and.Reed.pdf> Last accessed February 27, 2018.

Loucks, R. G., R. M. Reed, S. C. Ruppel, and D. M. Jarvie, 2009, Morphology, genesis, and distribution of nanometer-scale pores in siliceous mudstones of the Mississippian Barnett Shale: Journal of Sedimentary Research, v. 79, p. 848–861, doi:10.2110/jsr.2009.092.

Loucks, R. G., R. M. Reed, S. C. Ruppel, and D. M. Jarvie, 2012, Spectrum of pore types and networks in mudrocks and a descriptive classification for matrix-related mudrock pores: American Association of Petroleum Geologists Bulletin, v. 96, p. 1071–1098, doi:10.1306/08171111061.

Loucks R. G., and S. C. Ruppel, 2007, Mississippian Barnett Shale: Lithofacies and depositional setting of a deepwater shale-gas succession in the Fort Worth Basin, Texas: American Associa-

tion of Petroleum Geologists Bulletin, v. 91, p. 597–601, doi:10.1306/11020606059.

Meyer, B. D., 2002, Conodont biostratigraphy of Devonian strata of West Texas and eastern New Mexico and the apparatus of Early Devonian Icriodus species: Ph.D. Dissertation, Texas Tech University, Lubbock, 164 p, <https://ttu-ir.tdl.org/ttu-ir/handle/2346/13460> Last accessed February 27, 2018.

Miall, A. D., 2008, The southern midcontinent, Permian Basin, Ouachitas, *in* A. D. Miall, ed., The sedimentary basins of the United States and Canada: Elsevier B.V., Amsterdam, The Netherlands, p. 297–327, doi:10.1016/S1874-5997(08)00008-7.

Mulder, T., and J. Alexander, 2001, The physical character of subaqueous sedimentary density flows and their deposits: Sedimentology, v. 48, p. 269–299, doi:10.1046/j.1365-3091.2001.00360.x.

Noble, J. P., 1993, Paleooceanographic and tectonic implications of a regionally extensive Early Mississippian hiatus in the Ouachita system, southern mid-continental United States: Geology, v. 21, p. 315–318, doi:10.1130/0091-7613(1993)021<0315:PATIOA>2.3.CO;2.

Osterlund, C., 2012, The Barnett shale (Mississippian) in the central Midland Basin (Andrews, Ector, Martin, and Midland Counties): M.S. Thesis, Texas Christian University, Fort Worth, 76 p, <https://repository.tcu.edu/handle/116099117/4419> Last accessed February 27, 2018.

Pausé P. H., D. R. Adams, D. R., W. W. Collier, W. R. Gibson, H. A. Miller, L. D. Robbins, and S. M. Williams, 1985, Oil and
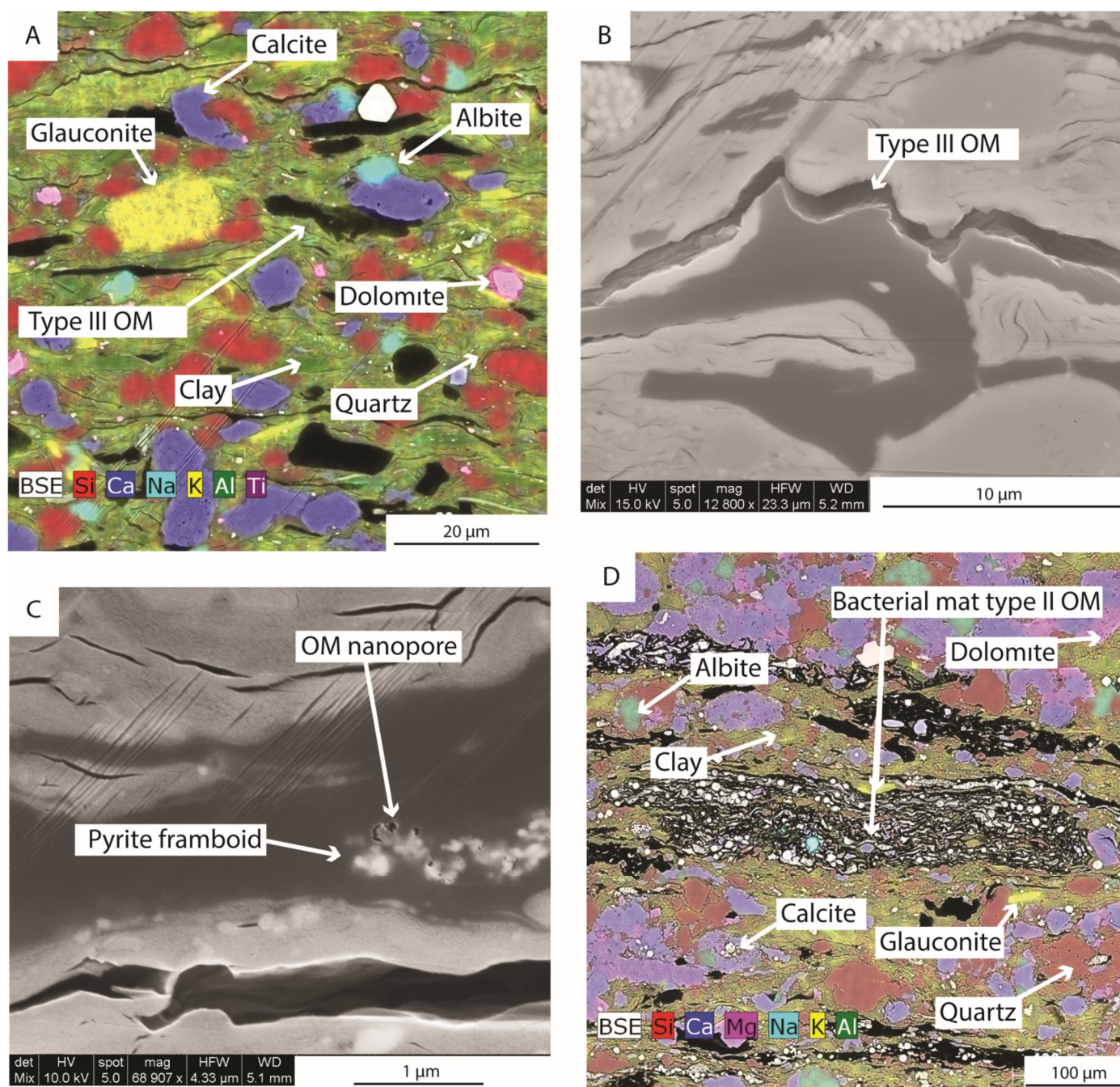
Figure 21. SEM EDS maps and images showing the organic-matter fraction of the Two Finger Sand. (A) EDS map of the argillaceous mudstone showing common type III organic matter (OM) structured nonporous organic matter; clay, calcite, dolomite, quartz, and glauconite are present. Lower Two Finger Sand: Anschutz Fasken 215B, 11,456 ft (~3491 m). (B) Type III organic matter (OM) displaying rigid framework and no organic-matter pores. Lower Two Finger Sand: Anschutz Fasken 215B, 11,456 ft (~3491 m). (C) Type III organic matter (OM) with inherited nanopores associated with pyrite. Lower Two Finger Sand: Anschutz Fasken 215B, 11,490 ft (~3502 m). (D) EDS map of the burrowed to laminated lime argillaceous siliceous packstone showing type II bacterial-mat-derived organic matter (OM); clay, calcite, dolomite, albite, glauconite, and quartz are present. Lower Two Finger Sand: Anschutz Fasken 215B, 11,455 ft (~3491 m).

gas developments in West Texas and eastern New Mexico in 1984: American Association of Petroleum Geologists Bulletin, v. 69, p. 1580–1587, <http://archives.datapages.com/data/bulletns/1984-85/images/pg/00690010/1550/15800.pdf> Last accessed February 27, 2018.

Reed, R. M., and R. G. Loucks, 2007, Imaging nanoscale pores in the Mississippian Barnett Shale of the northern Fort Worth Basin (abs.): American Association of Petroleum Geologists Search and Discovery Article 90063, Tulsa, Oklahoma, 1 p.,

<http://www.searchanddiscovery.com/abstracts/html/2007/annual/abstracts/lbReed.htm> Last accessed February 27, 2018.

Reed, R. M., and S. C. Ruppel, 2014, Variability in organic matter pore development over depth (abs.): A case study from the Devonian Woodford Formation, Delaware Basin, West Texas: American Association of Petroleum Geologists Search and Discovery Article 90189, Tulsa, Oklahoma, 1 p. <http://www.searchanddiscovery.com/abstracts/html/2014/90189ace/abstracts/1842072.html> Last accessed February, 26, 2018.
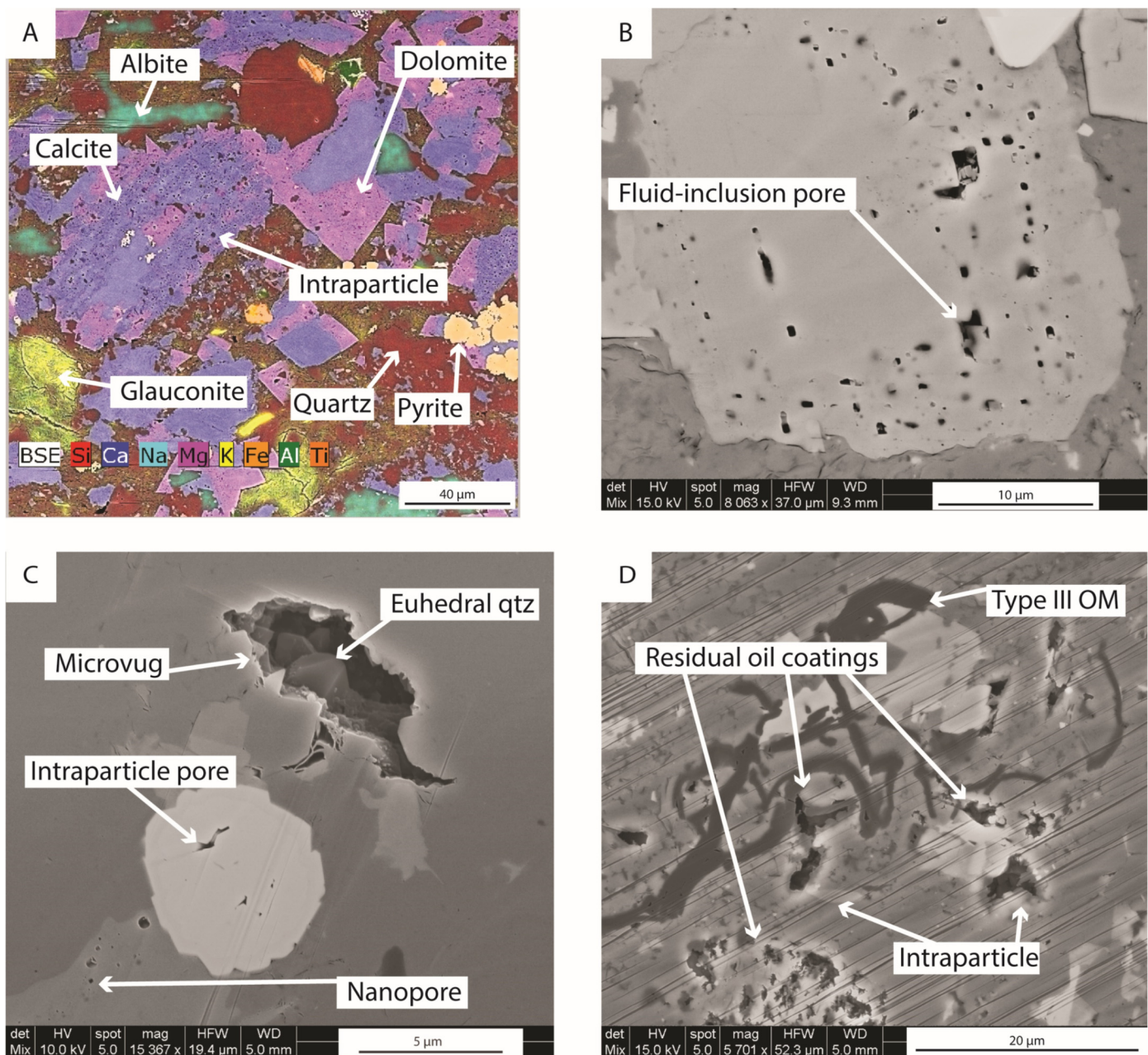
Figure 22. EDS and SEM images showing the pores observed in the Two Finger Sand. (A) EDS map of the burrowed to laminated siliceous lime packstone showing common intraparticle nano- to micropores within the carbonate grains and the dolomite rims. Glauconite also displays intraparticle nano- to micropores. Lower Two Finger Sand: Anschutz Fasken 215B, 11,475 ft (~3497.5 m). (B) Calcite grain with well-developed intraparticle fluid-inclusion pores ranging from nano- to micropores. Lower Two Finger Sand: Anschutz Fasken 215B, 11,521.5 ft (~3511.7 m). (C) Pyrite framboid with intraparticle nanopores and also a microvug intraparticle pore in matrix. Lower Two Finger Sand: Anschutz Fasken 215B, 11,521.5 ft (~3511.7 m). (D) Type III organic-matter (OM) in a quartz matrix showing intraparticle micropores with a residual oil coating. Lower Two Finger Sand: Anschutz Fasken 215B, 11,521.5 ft (~3511.7 m).

Ross, C. A., and J. R. P. Ross, 1987, Late Paleozoic sea levels and depositional sequences, *in* C. A. Ross and D. Haman, eds., Timing and deposition of eustatic sequences: Constraints on seismic stratigraphy: Cushman Foundation for Foraminiferal Research Special Publication 24, Lawrence, Kansas, p. 137–149, <https://cedar.wwu.edu/cgi/viewcontent.cgi?article=1060&context=geology_facpubs> Last accessed February 27, 2018.

Rowe, H. D., R. G. Loucks, S. C. Ruppel, and S. M. Rimmer, 2008, Mississippian Barnett Formation, Fort Worth Basin, Texas: Bulk geochemical inferences and Mo–TOC constraints on the severity of hydrographic restriction: Chemical Geology, v. 257, p. 16–25, doi:10.1016/j.chemgeo.2008.08.006.

Ruppel, S. C., 1985, Stratigraphy and petroleum potential of pre-Pennsylvanian rocks, Palo Duro Basin, Texas Panhandle: Texas Bureau of Economic Geology Report of Investigations 147, Austin, 81 p, <https://store.beg.utexas.edu/reports-of-investigations/1110-ri0147.html> Last accessed February 27, 2018.

Ruppel, S. C., and J. Kane, 2007, The Mississippian Barnett Formation: A source-rock seal and reservoir produced by Early Carboniferous flooding of the Texas Craton: Texas Bureau of
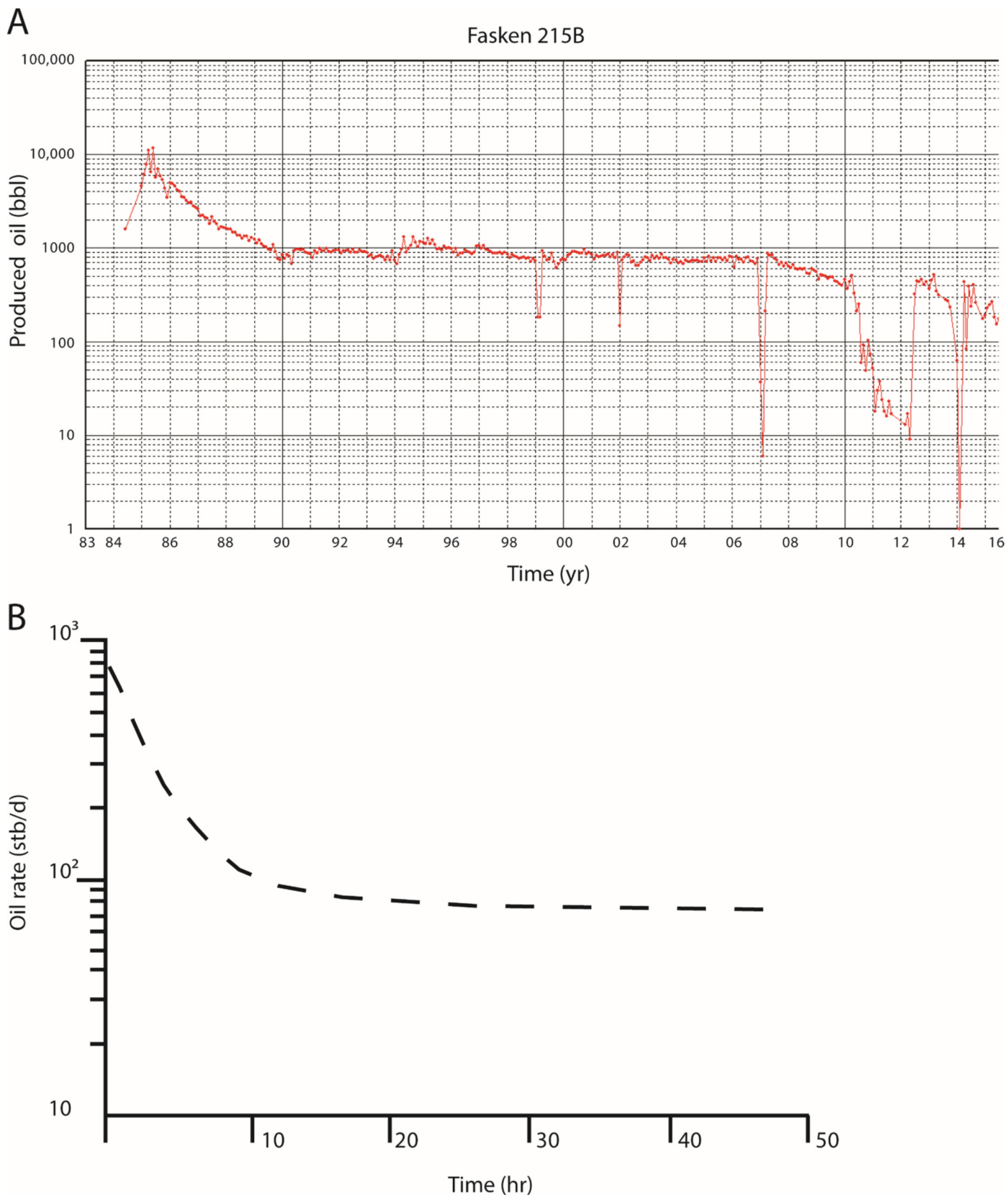
Figure 23. Comparison of the Anschutz Fasken 215B well to a simulated pressure drawdown in a naturally fractured reservoir. (A) Decline-curve analysis from the Anschutz Fasken 215B well. (B) Simulated pressure drawdown for a naturally fractured reservoir (modified after Blasingame and Lee, 1986). Note the rapid initial decline that represents initial production from fractures, followed by a steady and more uniform decline curve that occurs when the well starts to predominately produce from the low-permeability intraparticle pores (Candelaria, 1990).

Economic Geology Unpublished Report, Austin, 41 p., <http://www.beg.utexas.edu/files/content/beg/research/pbSyn/writ_synth/Mississippian_chapter.pdf> Last accessed February 27, 2018.

Sivils, D. J., 2004, An upper Mississippian carbonate ramp system for the Pedregosa Basin, southwestern New Mexico, U.S.A.: An outcrop analog for middle Carboniferous carbonate reservoirs, *in* G. M. Grammer, P. M. Harris, and G. P. Eberli, eds., Integration of outcrop and modern analogs in reservoir modeling: American Association of Petroleum Geologists Memoir 80, Tulsa, Oklahoma, p. 109–128, <http://archives.datapages.com/data/specpubs/memoir80/CHAPTER6/IMAGES/CHAPTER6.PDF> Last accessed February 27, 2018.

Yurewicz, D. A., 1977, Sedimentology of Mississippian basin-facies carbonates, New Mexico and West Texas; the Rancheria Formation, *in* H. E. Cook and P. Enos, eds., Deep-water carbonate environments: Society of Economic Paleontologists and Mineralogists Special Publication 25, Tulsa, Oklahoma, p. 203–219, <http://archives.datapages.com/data/sepm_sp/SP25/Sedimentology_of_Mississippian.pdf> Last accessed February 27, 2018.